Progress in Oceanography 206 (2022) 102854

Contents lists available at ScienceDirect

Progress in Oceanography

journal homepage: www.elsevier.com/locate/pocean

Dissolved organic carbon and nitrogen cycling along the west Antarctic Peninsula during summer

Ribanna Dittrich [a,*], Sian F. Henley [a], Hugh W. Ducklow [b], Michael P. Meredith [c]

[a] University of Edinburgh, UK
[b] Lamont Doherty Earth Observatory, USA
[c] British Antarctic Survey, UK

ARTICLE INFO

Keywords:
Nitrogen cycling
Biogeochemistry
West Antarctic Peninsula
Stable isotopes
Dissolved organic matter
Sea ice

ABSTRACT

The cycling of dissolved organic matter in the productive west Antarctic Peninsula (WAP) region is not well understood. For this study, dissolved organic carbon (DOC) and nitrogen (DON) concentrations and other biogeochemical measurements were collected along the WAP shelf during austral summer 2017. Concentrations of both DOC and DON in the upper ocean were lower than in lower latitudes (38.13–48.00 μmol C L^{-1}, 2.90–10.52 μmol N L^{-1}). DOC is produced along with particulate organic carbon during primary production, and is subsequently consumed by bacteria. DON shows high variability and is more likely the product of bacterial activity only in the surface waters. The N-isotopic composition of nitrate and particulate nitrogen showed intense nitrification, especially along the coast, and supports the findings of intense upper ocean cycling of organic matter of both particulate and dissolved forms. Export of DOM from the productive surface layer was negligible in the shelf waters of the WAP. Samples from glacial melt areas showed increased DON concentrations (7.88–10.52 μmol N L^{-1}) so we conclude that increasing warming and continuing melting of Antarctic glaciers may lead to higher concentrations of dissolved organic matter but also higher bacterial activity with more intense upper-ocean carbon and nitrogen cycling.

1. Introduction

1.1. Dissolved organic matter and climatic relevance in the Southern Ocean

Marine dissolved organic matter (DOM) plays a vital role in the global carbon cycle, yet processes driving the cycling of DOM are still poorly understood, particularly in the Southern Ocean. Bioavailable DOM is reworked and transformed by microbes (Carlson and Hansell, 2015; Jiao et al., 2010; Jiao et al., 2011) until it reaches a recalcitrant state. Throughout the global ocean, there is a pool of refractory DOM which, following the thermohaline circulation, becomes slightly depleted over time (Hansell, 2002). Hence, understanding how DOM is processed by microbes in the ocean is an important step in understanding the mechanisms involved in DOM cycling.

The Southern Ocean is estimated to be responsible for around 30% of the global atmospheric carbon uptake (Takahashi et al., 2009; Lenton et al., 2013; Gruber et al., 2009; Roobaert et al., 2019) with subsequent partial utilisation of this inorganic carbon by primary producers. Most of the open Southern Ocean is considered low in primary productivity (Tagliabue et al., 2014; Coale, 2004; Bowie et al., 2001; Boyd et al., 2007; Boyd and Ellwood, 2010) but the Antarctic shelf seas (such as the West Antarctic Peninsula; WAP) show increased primary production in comparison (e.g. up to 1100 mg C m^{-2} d^{-1} in Vernet et al., 2008). The region west of the Antarctic Peninsula is the most accessible part of Antarctica, which makes it a well-measured area compared to other Antarctic regions (e.g. studies of the U.S. Palmer Antarctica Long-Term Ecological Research (PAL LTER) Program and studies from the UK Rothera Research Station, Henley et al., 2019 and references therein).

At the WAP, the dynamics of DOM cycling are clearly distinguished from those found in lower latitude continental shelf seas, since allochthonous and anthropogenic sources are negligible due to minimum terrestrial river runoff or human impact so the major DOM source is *in situ* production (Billen and Becquevort, 1991). Organic matter dynamics in high latitude regions are ultimately controlled by light availability and climatic variations that exert control on the time-

Abbreviations: DOM, Dissolved Organic Matter; DOC, Dissolved Organic Carbon; DON, Dissolved Organic Nitrogen; WAP, West Antarctic Peninsula.

* Corresponding author at: University of Edinburgh, School of GeoSciences, Grant Institute, The King's Buildings, James Hutton Road, Edinburgh EH9 3FE, UK.
E-mail address: Ribanna.Dittrich@gmail.com (R. Dittrich).

https://doi.org/10.1016/j.pocean.2022.102854
Received 20 September 2021; Received in revised form 23 June 2022; Accepted 5 July 2022
Available online 9 July 2022

varying distribution of sea-ice (Saba et al., 2014). With increasing light availability and the start of sea-ice melt in the austral spring, high-biomass phytoplankton blooms develop over the summer season (Moline and Prezelin, 1996) with an increasing cross-shelf trend following the retreat of the sea-ice (Arrigo et al., 2017; Li et al., 2016). The phytoplankton community at the WAP during summer blooms is mostly dominated by diatoms, with a more minor contribution of other, mostly smaller, phytoplankton species (Moline et al., 2004; Montes-Hugo et al., 2009; Schofield et al., 2017; Brown et al., 2021) with studies suggesting a shift to a dominance by smaller species with warming (Ferreira et al., 2020; Russo et al., 2018; Lima et al., 2019). Locally (and depending on the water-column structure, but especially in regions with influence from other water masses such as the northern part of the WAP), phytoplankton blooms may be dominated by other, smaller species such as cryptophytes (Pereira et al., 2018). Bacterial decomposition with intense molecular restructuring of organic matter and preferential uptake of nitrogen (N) are thought to lead to the post-primary production release of DOM of varying quality (Caron et al., 1985; Goldman and Dennett, 2000; Pomeroy et al., 2007; Jiao et al., 2010; 2011).

1.2. Oceanographic and climatic context

The Antarctic Circumpolar Current (ACC) lies in close proximity to the WAP shelf. The southern boundary of the ACC is located on the upper continental slope between 750 and 1000 m depth. Intrusions of Upper Circumpolar Deep Water (UCDW) from the ACC penetrate onto the shelf, especially along deep glacially-scoured canyons; these provide a persistent source of warmer water (Martinson and McKee, 2012) with high nutrient and DIC concentrations (Klinck et al., 2004; Prézelin et al., 2000). Effective vertical mixing of UCDW with Antarctic Surface Water (AASW) provides the WAP surface waters with heat, salinity and nutrients (Meredith et al., 2013). These oceanographic characteristics make the WAP an ecologically and biogeochemically unusual region compared with other Antarctic shelf regions, many of which are typified by persistently colder, more homogeneous water columns.

The AASW at the WAP has a deep (~100 m) mixed layer in winter, and is comparatively saline and cold due to winter cooling and sea-ice formation (Clarke et al., 2008). During spring and summer, the surface waters become fresher and warmer due to ice melt and solar radiation, so that the deeper components of the winter AASW become isolated from the surface and exists as a subsurface remnant Winter Water (WW) layer, usually between 50 and 150 m depth (Meredith et al., 2013).

In the second half of the 20th century, the WAP exhibited rapid warming with increases in atmospheric and oceanic temperatures; changes in precipitation; a decline in sea-ice extent and duration; and increasing glacial melting in the area (Marshall et al., 2006; Vaughan et al., 2003; Van Wessem et al., 2015; Smith et al., 1996). Sea ice dynamics exert a leading-order influence on ecological processes in this region; accordingly the WAP ecosystem is subject to large intra- and inter-annual variability. Sea ice cover and duration at the WAP are strongly controlled by climatic variability, including the Southern Annular Mode (SAM; the dominant circumpolar mode of interannual climate variability in the extratropical Southern Hemisphere) and the El Niño-Southern Oscillation (ENSO). Interaction of these modes influences the location and depth of the Amundsen Sea Low (ASL), a low pressure system that resides between the WAP and the Ross Sea. Combined, these modes exert a strong influence on wind patterns at the WAP, and hence on the motion, phenology and distribution of sea ice (Stammerjohn et al., 2008; Saba et al., 2014; Vaughan et al., 2003).

The causes of the WAP warming since the middle of the last century are not known unambiguously, but potentially include enhanced teleconnections with the tropics, local feedbacks, and modifications in the circumpolar wind patterns. The warming trend is not monotonic, exhibiting periods of little change or even cooling. An apparent lack of warming since the turn of the 21st century has been attributed to natural variability superposed on the decadal warming trend (Turner et al., 2016).

Glacial meltwater supports stratification in coastal regions and has been shown to introduce micronutrients to the surface waters enhancing primary production (Annett et al., 2015; Eveleth et al., 2017). The effect of sea-ice melt and glacial meltwater on stratification has cascading effects on primary production and phytoplankton species composition: diatoms have been shown to grow more efficiently in shallower mixed layers due to enhanced irradiance, while haptophytes are often associated with areas of strongly mixed surface waters (Arrigo 1999) and cryptophytes occur with high glacial meltwater input (Moline et al., 2004).

1.3. Isotopic insights into nitrogen cycling in the west Antarctic Peninsula region

The stable isotope composition of nitrogen ($\delta^{15}N$) in nitrate and particulate nitrogen is used here to examine the upper ocean processes involved in the cycling of inorganic and organic nitrogen-containing compounds; for example, uptake of nitrate and ammonium, remineralisation and nitrification. $\delta^{15}N$ is defined as the deviation of the $^{15}N/^{14}N$ ratio in the sample from that of a universal reference standard atmospheric N_2 expressed in the per mille (‰) notation (equation (1)).

$$\delta^{15}N\ (‰) = \left(\frac{(\ ^{15}N/\ ^{14}N)_{\ sample}}{(\ ^{15}N/\ ^{14}N)_{\ standard}} - 1 \right) \times 1000 \quad (1)$$

Variations in the N-isotope composition of nitrate ($\delta^{15}N_{NO3}$), as the primary nitrogen source to Antarctic shelf surface waters, and particulate nitrogen ($\delta^{15}N_{PN}$) occur due to kinetic fractionation between the ^{14}N and ^{15}N isotopes caused by biological processes (see supplement 1). Uptake and assimilation of nitrate by phytoplankton favour the lighter ^{14}N isotope such that $\delta^{15}N_{NO3}$ in the water increases as nitrate utilisation proceeds. The degree of fractionation is defined by the fractionation factor or kinetic isotope effect (ε). ε is the ratio of the rates at which the two N isotopes are converted from nitrate to organic nitrogen.

Replenishment of the surface nitrate pool by nutrient-rich UCDW, sea-ice melt, organic matter remineralisation and nitrification can all cause deviations from modelled values of $\delta^{15}N_{NO3}$. As $\delta^{15}N_{PN}$ is influenced by $\delta^{15}N$ of the inorganic N source at the time of PN production as well as processes impacting on PN once it has been produced, $\delta^{15}N_{PN}$ is an integrative measurement that reflects the availability and uptake of different N sources and the remineralisation and loss processes underway.

1.4. Objectives

Future projections for the WAP show a potential shift to a food web in which microbial processing of organic matter plays a more important role, leading to higher DOM production but potentially also consumption (Sailley et al., 2013; Saba et al., 2014). While an increase in DOM production can lead to an increase in carbon export, it can also create a positive feedback mechanism by increasing upper-ocean respiration if this fresh DOM is bioavailable.

To determine how much DOM is available for export and/or recycled in this region and how these estimates vary and may change in the future, it is essential to understand the cycling of organic carbon and nitrogen.

The objective of this study is to understand how DOC and DON are being produced, utilised, remineralised and/or exported in this region seasonally with phytoplankton productivity as the ultimate DOM source. Dissolved and particulate organic carbon and nitrogen concentrations were analysed alongside other biogeochemical parameters including primary production, chlorophyll-*a* concentrations, bacterial abundance and production, inorganic nutrient concentrations and the N-isotopic

composition of nitrate and particulate nitrogen as part of the PAL LTER Program summer cruise in January 2017. This study advances our understanding of DOM cycling in high-productivity Antarctic shelf environments and its importance in larger-scale Southern Ocean biogeochemistry.

2. Materials and methods

2.1. Study region

The study area is part of the annually-sampled PAL LTER survey grid west of the Antarctic Peninsula (Ducklow et al., 2013) covering an area of 400 × 200 km. The sampling pattern consists of stations positioned along transect lines orthogonal to the coast approximately 100 km apart (Fig. 1). It is differentiated between off-shelf stations ("O", xxx.200), shelf stations ("S", xxx.100), coastal stations ("C", xxx.040 or xxx.060) and one inshore station ("I", 200.000). For this study, samples were collected from January 6th to January 31st 2017 on board the *ARSV Laurence M. Gould*. The sampling scheme on each annual cruise involves deployments of a SeaBird 911 + conductivity-temperature-depth instrument attached to a 24-bottle Niskin bottle rosette used to collect seawater samples over the full water column depth. Sea-ice data are derived from satellite observations from NASA's Scanning Multichannel Microwave Radiometer and the Defense Meteorological Satellite Program's Special Sensor Microwave/Imager (Stammerjohn et al., 2008). Days since sea-ice retreat are defined as the number of days since sea-ice cover was <15% for at least 5 consecutive days (Stammerjohn et al., 2008).

2.2. Sample collection

At each sampling station, samples for DOC, total dissolved nitrogen (TDN), inorganic nutrients, N-isotopic composition of nitrate and bacterial measurements were collected in acid-cleaned 60-ml HDPE bottles. Sampled seawater was gravity-filtered directly from the Niskin bottles through pre-combusted GF/F filters (Whatman 0.7 μm nominal pore size, 47 mm Ø) and immediately transferred to a −80 °C freezer. POM samples were collected from the top 6 sampling depths at every station by filtering up to 4 L of collected seawater through pre-combusted GF/F filters (Whatman 0.7 μm GF/F 25 mm Ø). The filters were stored in cryovials at −80 °C. Primary production and chlorophyll-*a* samples were collected directly from Niskin bottles into brown HDPE bottles. Samples for $\delta^{18}O_{H2O}$ analysis were collected in 50-ml glass bottles which were stoppered and crimp-sealed.

2.3. Analysis of bulk dissolved organic carbon and nitrogen concentrations

DOC and TDN analyses were conducted via high-temperature combustion on a *Shimadzu TOC-V Analyser* with an attached *TNM1 Total Nitrogen Measuring unit*. 10 mL of each sample was transferred into acid-cleaned and combusted glass vials using an acid-cleaned 5 mL pipette. Sample replicates were analysed in each run to measure analytical precision. Certified Reference Material (D.M. Hansell Lab, Univ. of Miami) was analysed before and after each batch of samples to determine the accuracy of the analytical method. CRMs were processed with each sample set to ensure linearity of the instrument throughout the period of analysis. Detection limits were 0.04 μmol C L^{-1} for DOC and 0.36 μmol N L^{-1} for TDN, and analytical precision for DOC was ± 1.09 μmol C L^{-1} and for TDN ± 0.51 μmol N L^{-1}.

DON concentrations were calculated by subtracting inorganic nitrogen species concentrations from TDN. Due to logistical constraints, samples from the PAL LTER cruise were only analysed for the inorganic nitrogen species NO_2^- and NO_3^- so that the DON concentrations presented here also include NH_4^+, consistent with other studies of DOM concentrations from the Palmer LTER. NH_4^+ concentrations in WAP surface waters have been shown to be minimal at the beginning and for the period of intense primary production (Henley et al., 2018; Serebrennikova and Fanning, 2004; Serebrennikova, 2005); however, when NH_4^+ concentrations might be of importance, they are mentioned in the discussion.

2.4. Inorganic nutrient analysis

Dissolved inorganic nutrient concentrations (nitrate + nitrite, silicic acid and phosphate) were analysed using a *Seal Analytical* segmented flow autoanalyser using standard protocols (Mequon, WI, Seal AutoAnalyzer AA3; SEAL Analytical, Inc. 2019) at Lamont Doherty Earth Observatory, USA. A deep-sea sample from 3,000 m was analysed as an internal reference standard. Detection limits were 0.015 μmol N L^{-1} for nitrate + nitrite, 0.0021 μmol P L^{-1} for phosphate and 0.03 μmol Si L^{-1} for silicic acid.

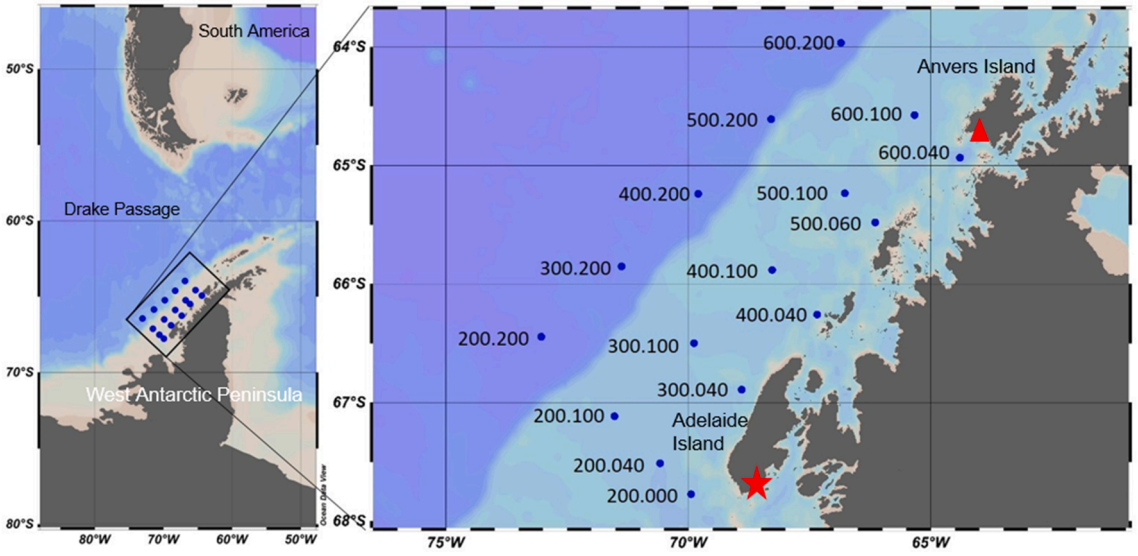

Fig. 1. The PAL LTER annual sampling stations west of the Antarctic Peninsula. The numbers at each sampling station show the sampling station names. ★ = UK Rothera Research Station ▲ = US Palmer Station.

2.5. Analysis of particulate organic carbon and nitrogen concentrations and the N-isotopic composition of particulate nitrogen

The concentrations of POC and PN and the stable isotopic composition of PN were analysed at the School of GeoSciences at the University of Edinburgh. Filters for POC and PN analysis were prepared following a method adapted from Lourey et al. (2004). Samples were analysed on a CE Instruments NA2500 Elemental Analyser inline with a Thermo Finnigan Delta + Advantage stable isotope ratio mass spectrometer (IRMS). Both instruments are linked through a Finnigan ConFlo III Universal Interface to allow for simultaneous carbon and nitrogen analysis. The certified reference materials PACS-2 and acetanilide were analysed for the isotopic composition and carbon and nitrogen concentrations, respectively. The N-isotopic composition is presented in the delta per mille notation relative to the international standard atmospheric N_2 ($\delta^{15}N‰_{AIR}$). The analytical precision was better than 1.0% wt for POC, better than 1.1% wt for PN and 0.2‰ for $\delta^{15}N_{PN}$.

2.6. Analysis of N-isotopic composition of NO_3^- via the denitrifier method

Analysis of the N-isotopic composition of NO_3^- followed the denitrifier method, wherein nitrate is converted to N_2O by the denitrifying bacteria *Pseudomonas aureofaciens* (Sigman et al., 2001; Casciotti et al., 2002; Tuerena et al., 2015). Nitrite was not removed prior to denitrification, so the $\delta^{15}N_{NO3}$ values reported here are $\delta^{15}N$ of the combined nitrate + nitrite pool. Seawater samples were injected into aliquots of nitrogen-purged bacterial media with a gas-tight syringe and left to denitrify overnight. Samples were then injected with 10 N sodium hydroxide to lyse bacteria, stop the denitrification reaction and scavenge CO_2. Samples were analysed by headspace analysis using a Combi PAL auto-sampler linked to a Thermo Fisher Scientific GasBench II system and Thermo Fisher Scientific Delta + Advantage IRMS. The N-isotopic composition is presented in the delta per mille notation relative to the international standard atmospheric N_2 ($\delta^{15}N‰_{AIR}$) by referencing raw data to isotopic standards USGS-32, USGS-34 and USGS-35. The analytical precision is 0.2‰ for $\delta^{15}N_{NO3}$.

2.7. Bacterial measurements

Bacterial abundance, production and HNA/LNA (high nucleic acid and low nucleic acid cells) were analysed onboard the ship. Bacterial abundance and HNA and LNA were analysed within two hours of collection via flow cytometry on a Becton-Dickinson Accuri C6 instrument following Gasol and Del Giorgio (2000). Bacterial production rates were determined via incorporation of ^{3}H-labelled leucine following a protocol modified from Smith and Azam (1992). Samples were assayed in triplicate. Each 1.5 mL sample was inoculated with ^{3}H-leucine (MP Biomedical, Santa Ana, CA; >100 Ci/mmol, 20–25 nmol N L^{-1} final concentration) and incubated for 3 h at ± 0.5 °C of the *in situ* temperature. At the end of the incubation period, 200 μL 100% trichloroacetic acid was added to the samples to stop uptake. After concentration by centrifugation, the samples were rinsed with 5% trichloroacetic acid and 70% ethanol and air-dried overnight before analysis by liquid scintillation counting in an Ultima Gold cocktail on a Packard TriCarb instrument.

2.8. Primary production and chlorophyll-a measurements

Primary production rates, calculated as daily carbon uptake in mg C m^{-3} day^{-1}, were measured in deck incubators cooled with flowing seawater. 100 mL seawater samples were inoculated with 1 μCi of ^{14}C-labelled $NaHCO_3$ in borosilicate bottles. The bottles were incubated for 24 h at *in situ* light levels and ambient surface temperatures. After the 24-hour incubation period, the seawater samples were filtered through GF/F filters, the filters were washed with 10% HCl, dried and counted in a scintillation counter. Chlorophyll *a* samples were filtered onto GF/F filters and kept frozen at – 80 °C. Analysis was conducted at Palmer Station through acetone extraction and measurement of the extract on a Turner AU10 Fluorometer.

2.9. Analysis of stable oxygen isotopes in seawater ($\delta^{18}O_{H2O}$)

Samples were analysed for $\delta^{18}O_{H2O}$ at the Natural Environmental Research Council (NERC) Isotope Geosciences Laboratory at the British Geological Survey using a *VG Isoprep 18* and *SIRA 10* mass spectrometer. The method followed the equilibrium method for CO_2 established by Epstein and Mayeda (1953). A subset of samples was analysed in duplicate to assess precision; this was determined to be better than ± 0.02‰. Using the $\delta^{18}O_{H2O}$ and salinity data, the contributions of sea ice and meteoric water (glacial melt plus precipitation) to each of the samples collected were calculated using a set of mass balance equations, following Meredith et al. (2016) who adapted the method from Östlund and Hut (1984).

3. Results

3.1. Hydrography and sea ice

Salinity was most variable in the surface waters due to the combined effects of sea-ice melt and glacial meltwater (Fig. 2a). Surface water salinity was lowest at station 300.040, adjacent to Adelaide Island (32.64) and highest at station 300.200, beyond the shelf break (33.92). The influence of sea ice and glacial meltwater is revealed by comparing the spatial patterns of salinity (Fig. 2a) and $\delta^{18}O$ (Fig. 2d). The lowest $\delta^{18}O$-value coincides with the lowest salinity (300.040), revealing significant meteoric water input at this location. Mass balance calculations reveal 6.1% meteoric water at this location, presumed largely in the form of glacial discharge. A strong cross-shelf gradient in meteoric water percentage is apparent, with a minimum (2.1%) at station 400.200.

Sea-surface temperature (SST) in the LTER grid ranged from 1.1 to 2.9 °C (mean 2.1 ± 0.46 °C) (Fig. 2b). Highest SST was found in the north (stations 500.060 and 500.100 with 2.9°C and 2.7°C, respectively) and lowest SST in the coastal south (300.040 and 200.040 with 1.3°C and 1.1°C, respectively).

Sea ice retreated from the off-shelf area earliest (>100 days prior to sampling) and latest in the coastal regions (5 to 54 days prior to sampling). Fig. 2c shows the number of days between the sampling date and sea-ice retreat, which corresponds to the period over which the surface ocean has been exposed to the atmosphere and ambient levels of incoming solar radiation, prior to sampling.

3.2. Phytoplankton and bacteria

Surface primary production and chlorophyll-*a* concentrations show a similar cross-shelf gradient with highest values along the coast (Fig. 2f, 2g). Primary production peaked in the north at station 500.060 (101.9 mg C m^{-3} d^{-1}) while highest chlorophyll-*a* concentrations (16.98 mg m^{-3}) were found at 300.040. At the shelf and off-shelf stations, both primary production and chlorophyll-*a* concentrations were substantially lower, with primary production showing more variability and rates up to 55.2 mg C m^{-3} d^{-1} at 400.100 while chlorophyll-*a* generally stayed below 1.83 mg m^{-3}.

Highest bacterial leucine incorporation rates occurred at the coastal stations, decreasing off the shelf and towards the north (Fig. 2h, Fig. 3). Bacterial abundance peaked at stations 200.000 and 300.040 while leucine incorporation peaked at 200.000 and 400.040. In relation to the rest of the sampling grid, leucine incorporation maxima at these stations were extremely high at > 400 pmol leu hr^{-1} L^{-1}. Other surface values showed high variability ranging from leucine incorporation rates as low as 3.65 pmol leu hr^{-1} L^{-1} at 200.200 to 168.3 pmol leu hr^{-1} L^{-1} at 300.040. All off-shelf stations showed leucine incorporation maxima at depths between 25 and 30 m; at almost all coastal stations (except

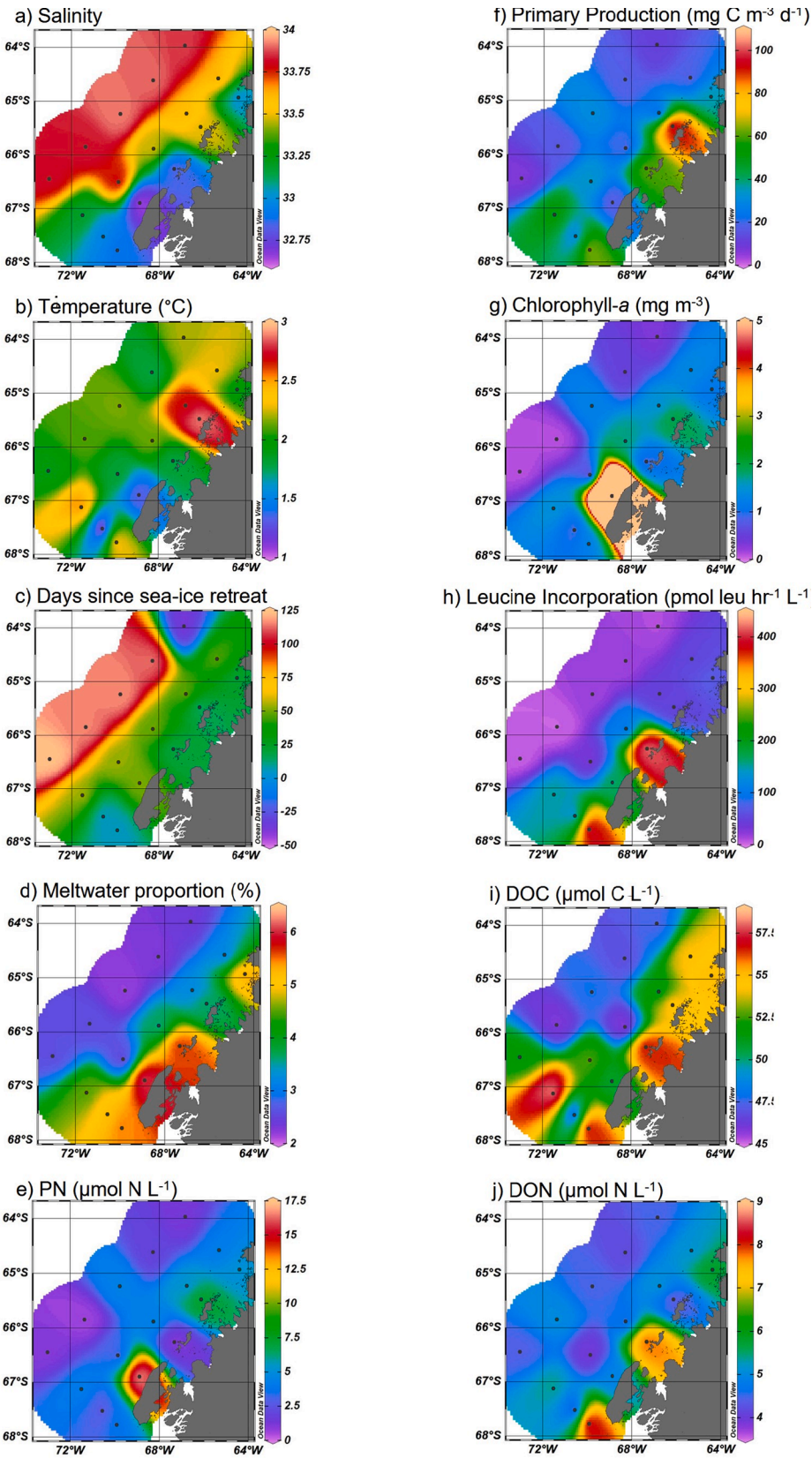

Fig. 2. Physical and biogeochemical surface conditions for the PAL LTER grid in January 2017. Panels show (a) salinity, (b) sea surface temperature, (c) number of days since sea ice retreat, (d) $\delta^{18}O_{H2O}$, as well as concentrations of (e) PN, (g) chlorophyll *a*, (i) DOC* and (j) DON*, and rates of (f) primary production and (h) leucine incorporation (POC is not shown as the surface distribution is reflected in PN concentrations). *DOC and DON concentrations at station 300.040 are shown for 10 m depth as no surface data were available.

300.040) maxima were found at the surface. Leucine incorporation at the off-shelf stations was 10 to 100 times lower than along the coast, ranging from 0.36 pmol leu hr^{-1} L^{-1} at station 200.200 to 21.73 pmol leu hr^{-1} L^{-1} at station 400.200. Bacterial abundance showed high variability, with highest values along the coast ranging from $4.4x10^8$ cells L^{-1} at 500.100 to $3.1x10^9$ cells L^{-1} at 200.000. At the off-shelf stations, bacterial abundance peaks are deeper, mostly between 40 and 60 m, while at the shelf and coastal stations, highest bacterial

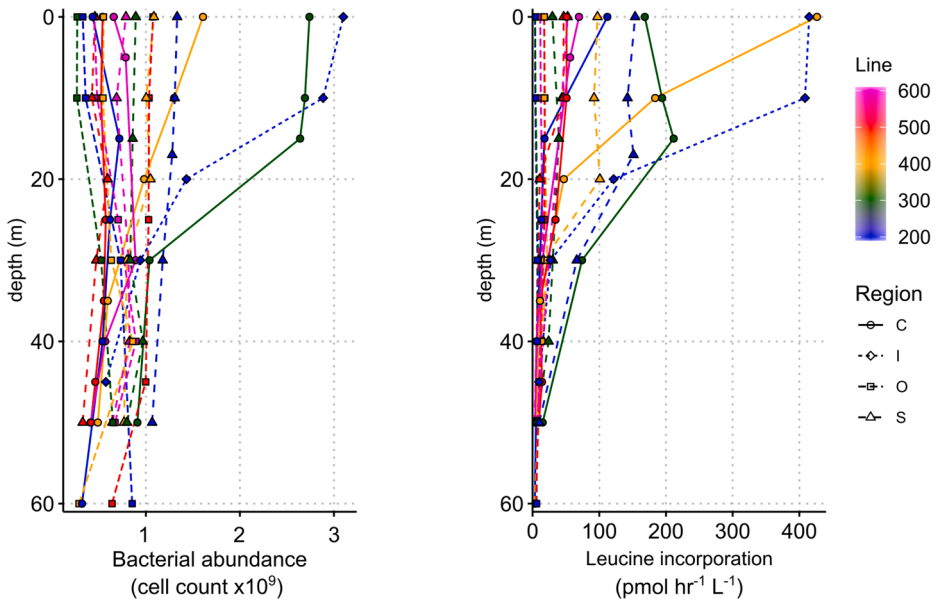

Fig. 3. Depth profile plots for bacterial abundance and leucine incorporation rates over the upper 60 m at stations across the Palmer LTER grid in January 2017. Stations are colour-coded by sampling grid line orthogonal to the WAP coast according to the colour legend, with coastal (C), inshore (I), off-shelf (O) and shelf (S) stations differentiated by symbol and line type according to the symbol legend.

abundance is mostly found at the surface or between 10 and 25 m. The ratio of HNA to LNA bacteria at the upper three depths ranged between 1.2 and 6.6 with the exception of stations 300.040 (10.7) and 200.000 (14.6).

3.3. Dissolved and particulate organic matter distribution

Across the entire PAL LTER sampling grid, highest DOC concentrations (>48 μmol C L^{-1}) were found mostly in the upper 20 m while DON maxima were found over the full range of sampled depths (Fig. 4). The coastal stations 200.000 and 400.040 showed high DON concentrations in the surface waters (8.70 μmol N L^{-1} and 7.88 μmol N L^{-1}, respectively; Fig. 2j). Lowest DOC concentrations were found at depths > 50 m and covered a narrow range from 38.13 to 40.88 μmol C L^{-1}. DON minima were mostly found at depths > 60 m with the exceptions of stations 500.200 and 600.200 where DON minima were found in the upper 25 m and DON maxima at 40 and 60 m, respectively.

Surface POC and PN concentrations were generally highest along the coast, ranging from 14.80 μmol C L^{-1} and 2.59 μmol N L^{-1} at station 200.040 to 98.62 μmol C L^{-1} and 16.84 μmol N L^{-1} at station 300.040 (Fig. 2e). C:N ratios of POM in the upper 15 m were around the Redfield ratio of 6.6 with a mean of 6.47 ± 0.37, except for stations 500.200, 600.200 and 600.100 (the stations that are farthest north and from the coast) where C:N ratios were higher (between 7.2 and 13). While PN concentrations decreased faster with depth than POC, driving increases in POC:PN ratios with depth, POC:PN ratios at the southern stations (all of the 200 line, 300.040 and 300.100) only vary slightly and mostly stay below 7 in the upper 50 m.

3.4. Nutrient concentrations

The surface distribution of inorganic nutrients across the sampling

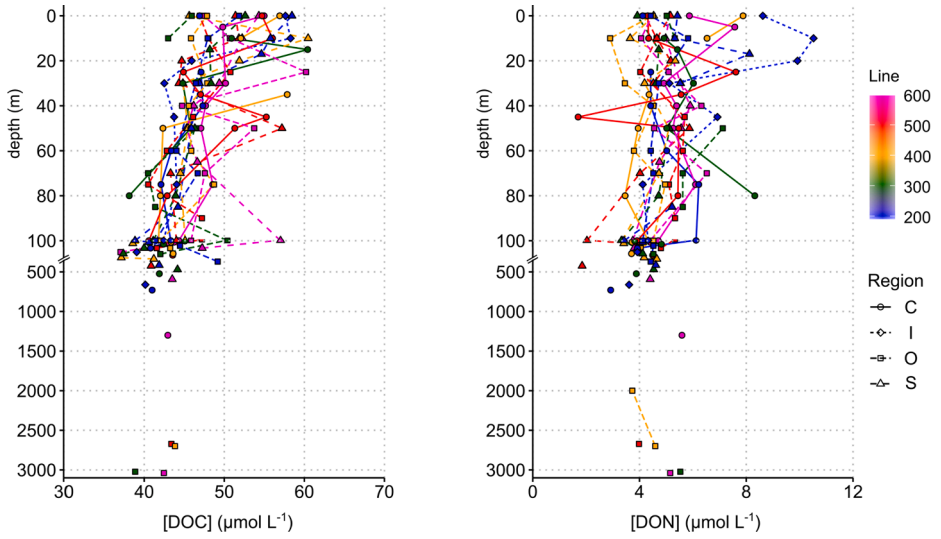

Fig. 4. Depth profile plots for DOC and DON concentrations over the full water column depth at stations across the Palmer LTER grid in January 2017. Note the break in y-axis scales at 105 m to show higher resolution for the upper 100 m. Stations are colour-coded by sampling grid line orthogonal to the WAP coast according to the colour legend, with coastal (C), inshore (I), off-shelf (O) and shelf (S) stations differentiated by symbol and line type according to the symbol legend.

grid reflects the physical conditions described above (Fig. 5). At depths > 200 m, NO_3^- concentrations had a mean value of 33.15 ± 1.21 μmol N L^{-1} representing NO_3^- concentrations in CDW being transported across the WAP shelf. Above 100 m, NO_3^- concentrations decreased towards the surface. Surface NO_3^- concentrations ranged from 0.77 μmol N L^{-1} at 300.040 to 25.45 μmol N L^{-1} at 200.200. The off-shelf stations showed higher surface concentrations (24.52 ± 1.26 μmol N L^{-1}) in comparison to shelf waters (19.34 ± 1.86 μmol N L^{-1}) and coastal stations (12.85 ± 6.6 μmol N L^{-1}). The higher standard deviation at the coastal stations shows more variable NO_3^- uptake in these waters with more depleted surface waters at the southernmost stations.

3.5. N-isotopic composition of NO_3^- and PN

The N-isotopic composition of NO_3^- and PN was highly variable across the sampling grid, with a clear distinction in both signatures between coastal, shelf and off-shelf stations. $\delta^{15}N_{NO3}$ was lowest in CDW (5.2 ± 0.3‰) and increased into the surface ocean as nitrate was drawn down, to values of > 6.5‰ in the upper 15 m at all stations. The highest values of $\delta^{15}N_{NO3}$ in the upper 15 m (>8‰) were observed at coastal stations 600.040, 500.060, 300.040, 200.000 and the shelf station 500.100. The lowest values of $\delta^{15}N_{NO3}$ in the upper 15 m (<7.3‰) were observed at off-shelf stations 600.200, 500.200, 300.200, 200.200 as well as the shelf station 200.040. $\delta^{15}N_{PN}$ also showed the highest values in the upper 15 m at coastal stations 500.060 and 300.040 (>6‰) as well as the shelf station 300.100 (>4‰), where POM concentration, chlorophyll-*a* and/or primary production were also high (Fig. 2f, 2g). At all other stations, $\delta^{15}N_{PN}$ values in the upper 15 m were between −2.5 and 3‰ with the lowest values at the off-shelf stations 400.200 and 200.200, shelf stations 600.100, 400.100, 200.100, and the coastal station 600.040. $\delta^{15}N_{PN}$ increases with depth below the mixed layer (between 20 and 110 m) at all stations, with the magnitude of this increase ranging from 2.5 to 7.2‰.

4. Discussion

4.1. Seasonal cycling of DOM along the WAP shelf

4.1.1. Spatial distribution of DOM

The measured deep-sea DOC and DON concentrations (taken at ~ 3000 m, CDW) analysed in this study were within a range of 38.87 to 42.45 μmol C L^{-1}, and 4.64 to 5.53 μmol N L^{-1}, respectively. These values are consistent with previous DOM studies in the Southern Ocean and represent deep water concentrations of refractory DOM (Carlson et al., 2000; 1998; Hubberten et al., 1995; Lechtenfeld et al., 2014; Nikrad et al., 2014; Sanders and Jickells 2000; Wang et al., 2010; Ogawa et al., 1999).

The predominant water masses in the study area are UCDW, LCDW, AASW and WW (Fig. 6, Emery and Meincke 1986; Martinson and McKee 2012; Carter et al., 2008, Klinck et al., 2004, Ducklow et al., 2007). The entrainment of UCDW towards the surface ocean along the WAP introduces refractory DOM and inorganic nutrients into the upper ocean (Pollard et al., 2006; Sigman et al., 1999) so that there is a constant background of refractory DOM concentrations. Concentrations of seasonally bioavailable (labile and semi-labile) DOC and DON can therefore be estimated by subtracting the deep-sea DOC and DON concentrations from upper ocean values (e.g. Soendergaard et al., 2000).

The surface DOC distribution across the entire LTER grid shows a cross-shelf trend with higher concentrations at the coastal stations; however, the values are patchy and highly variable. DON shows significant variability between coast and off-shelf stations (paired *t*-test t = 2.161, $p = 0.035$) with higher [DON] at the coastal stations than at the off-shelf stations.

4.1.2. DOC and DON dynamics as a result of phytoplankton bloom progression and bacterial response

The distributions of biological properties such as primary production and nutrients show a clear cross-shelf trend, which follows the physical changes of the WAP ecosystem triggered by the retreat of sea ice, and represents the annual cycle of primary production in the WAP shelf waters (e.g. Moline and Prezelin 1996; Ducklow, et al., 2012). Sea ice retreated earlier in the off-shelf region than closer to the shore, so that regions of open water could support phytoplankton blooms much earlier than in the coastal regions where sea ice only retreated shortly before sampling (Stammerjohn et al., 2008). Due to this timing difference, a progression in phytoplankton bloom development and the biogeochemical response can be observed across the shelf. DOM concentrations measured at the WAP have been lower than in other high-productivity regions of the global ocean (Carlson et al., 1998; Ducklow et al., 2008), and have been thought to be only the product of bacterial transformation of POM, which causes a time lag between peaks in POM and DOM concentrations (Carlson et al., 1998).

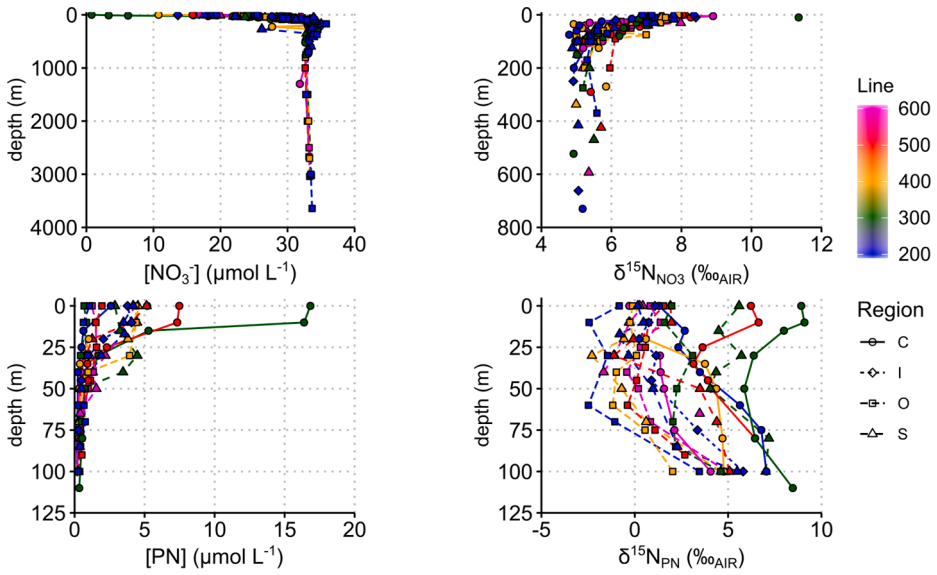

Fig. 5. Depth profile plots for the concentration and N-isotopic composition of nitrate and PN at stations across the Palmer LTER grid in January 2017. Note different y-axis scales between plots. Stations are colour-coded by sampling grid line orthogonal to the WAP coast according to the colour legend, with coastal (C), inshore (I), off-shelf (O) and shelf (S) stations differentiated by symbol and line type according to the symbol legend.

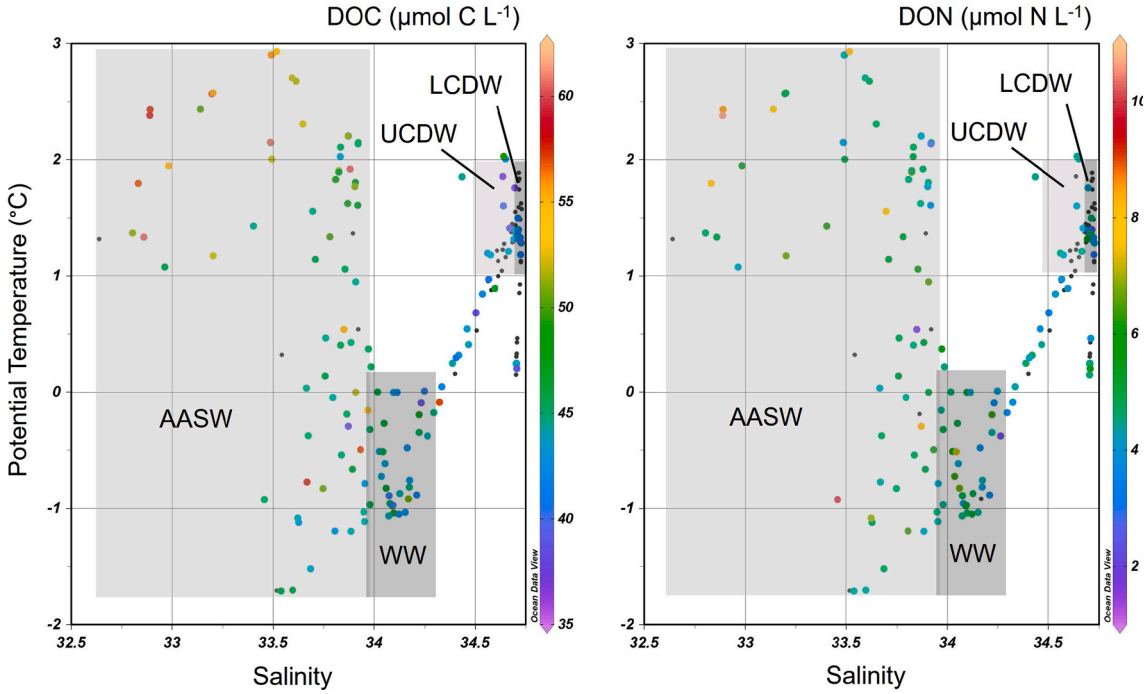

Fig. 6. Temperature-salinity plot with DOC (left panel) and DON concentrations (right panel) as the z variable for the entire study region. T-S fields for AASW, WW, UCDW and Lower CDW (LCDW) are depicted by grey shaded boxes as per annotations. UCDW and LCDW are as defined previously (Emery and Meincke, 1986; Martinson and McKee, 2012; Carter, McCave, and Williams, 2008). AASW and WW are adapted from Klinck et al. (2004), Ducklow et al. (2007) and Emery and Meincke (1986), to improve fit to our data. Grey data points show sample depths where DOM was not measured.

During the PAL LTER cruise in January 2017, peaks of labile DOC concentrations of > 10 µmol C L^{-1} above the refractory background levels were consistently found at the same depth as either the chlorophyll-*a* or bacterial activity maximum suggesting co-production of DOC during primary production and bacterial processes. DOC shows a significant albeit weak correlation with POC (r = 0.52, $p = 4.3*10^{-6}$) as well as NO_3^- concentrations (r = -0.55, p = 3.8 * 10^{-7}, Fig. 7), indicating direct production of DOC during primary production. These findings contrast with previous studies (Rozema et al., 2016; Ducklow et al., 2012; Billen and Becquevort 1991; Ghiglione and Murray 2012; Piquet et al., 2011) that suggest little to no direct DOC production or release during primary production, at least relative to the high primary production rates characteristic of this region.

There are no significant relationships between DON and phytoplankton parameters (Fig. 8, r2 < 0.2, p > 0.1) indicating that processes other than primary production are primarily responsible for DON production and removal. Surface [DON] showed significant positive correlations with both bacterial abundance ($r^2 = 0.65$, p = 3.1*10^{-4}) and leucine incorporation ($r^2 = 0.82$, p = 3.3*10^{-6}, Fig. 8), suggesting that DON is produced by bacterial processes. Although no comparable data are available for elsewhere in the Southern Ocean, these findings support the results of a DOM model study based on ^{13}C tracer experiments in

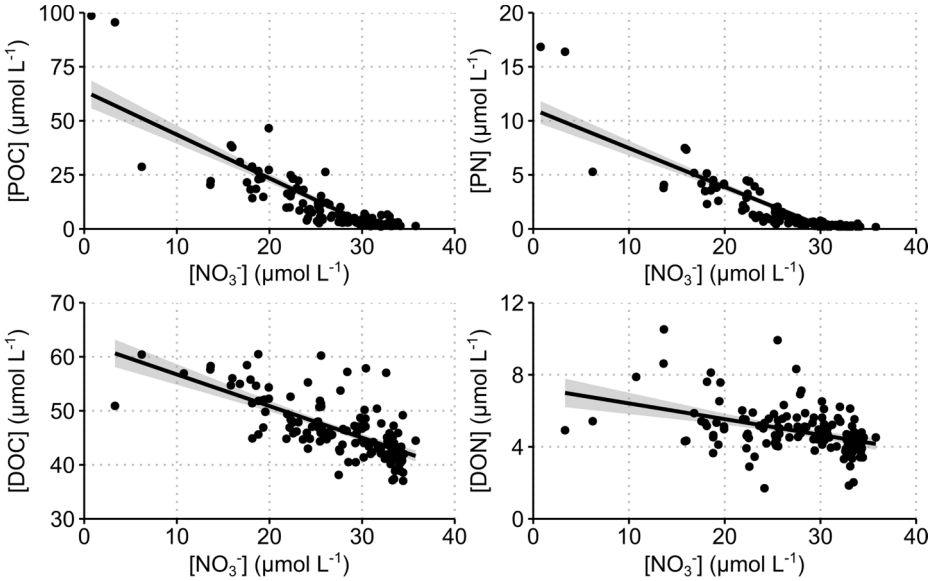

Fig. 7. Nitrate concentrations plotted against POC, PN, DOC and DON concentrations for stations across the Palmer LTER grid in January 2017. Statistically significant correlations are shown (black) with 95% confidence intervals (grey).

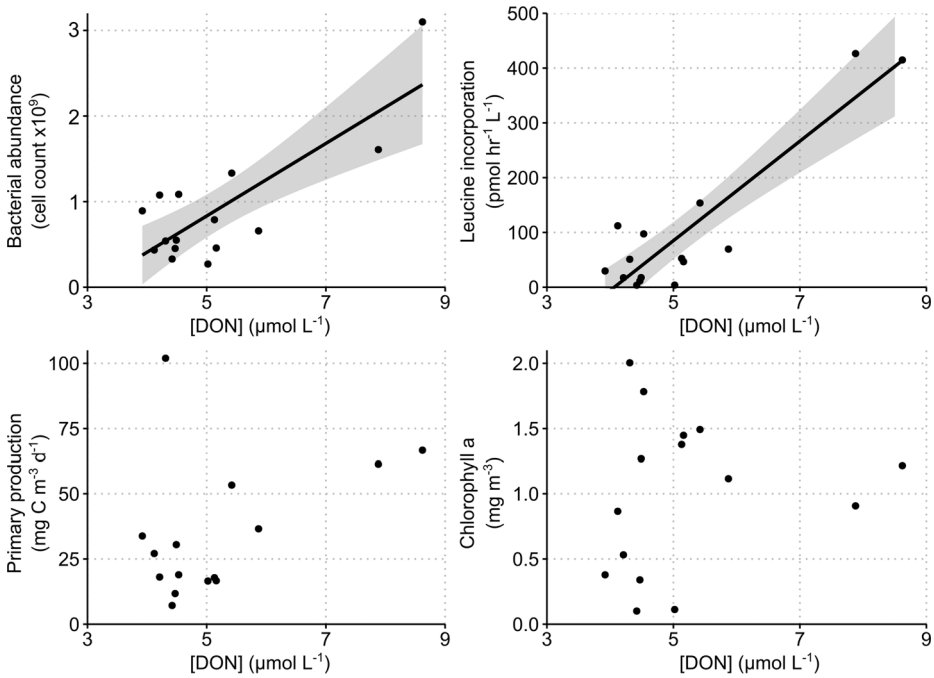

Fig. 8. Surface DON concentrations plotted against bacterial abundance, leucine incorporation rates, primary production rates and chlorophyll-a concentrations for stations across the Palmer LTER grid in January 2017. Statistically significant correlations are shown (black) with 95% confidence intervals (grey). Where no regression line is shown, the relationship is not statistically significant at the 95% confidence level.

a Danish fjord (Van den Meersche et al., 2004). Those authors found that 60% of DOC was released directly by phytoplankton and 40% by bacterial processes, while over 99% of DON is likely the product of bacteria. Time-series data collected from 2013 to 2016 in the coastal waters off Rothera Research Station on Adelaide Island in the central WAP (Fig. 1) suggest similar dynamics in DOC and DON production and consumption (Dittrich 2020).

Whilst carbon is not limiting in the ocean, nitrogen can become a limiting nutrient for phytoplankton, such that the direct release of N-containing DOM compounds by a healthy phytoplankton cell during a photosynthetic production period is accompanied by high energetic costs (Ward and Bronk 2001). In the Southern Ocean, nitrogen is not limiting in general, although in regions where primary production is not limited by iron or other co-limiting micronutrients for the most part, such as the WAP, inorganic nitrogen can be depleted to limiting levels, as we observed. Under these circumstances, DON released by phytoplankton might represent a valuable and bioavailable source of nitrogen for phytoplankton.

4.1.3. Efficient cycling of dissolved organic matter in the surface ocean of the WAP

DOC and DON concentrations decline to background concentrations within the top 50–150 m (Fig. 4). In combination with the significant relationship of DON with bacterial measurements in surface waters, these dynamics suggest that DOM cycling in the upper ocean is taking place efficiently, to such an extent that there is no or little export of DOM to depths below 50–60 m. In the upper 50 m, both [DOC] and [DON] are highly variable between stations, both horizontally and vertically. Below a depth of 50 m, [DOC] shows much less variability while and [DON] decreases slightly but remains variable. Elevated DON concentrations between 50 and 100 m at some stations are likely due to increased ammonium concentrations, which are a product of bacterial organic nitrogen degradation and were not measured during this research cruise. Increased post-primary production ammonium concentrations were shown in previous studies in the southern coastal waters of the WAP (Serebrennikova and Fanning, 2004b; Serebrennikova et al., 2008) but also during high rates of primary production in the same area (Dittrich, 2020).

The limited variability of DOC and DON and low concentrations below 50–150 m show efficient cycling of labile DOM in the upper ocean so that no or little DOM is being exported to depth.

Our particulate data (Fig. 5) further show that PN concentrations decline rapidly over the upper 50 m, such that both POM and DOM appear to be remineralised efficiently in the upper ocean, with limited export to depth. These findings build on previous studies showing that the WAP is a productive ecosystem but is inefficient in organic matter export, and support previous suggestions that horizontal advection may be a more efficient transport pathway for suspended organic matter (Ducklow et al., 2018; Stukel et al., 2015; Stukel and Ducklow, 2017). However, it might also show that upper-ocean carbon and nitrogen remineralisation occur efficiently for both POM and DOM.

4.2. Conceptual model of seasonal organic matter cycling at the WAP

Here we present a simple conceptual model to describe and summarise the progression of a phytoplankton bloom and associated biogeochemical cycling, including POM and DOM production and the development of the bacterial processes and communities (Fig. 9). Shortly after the retreat of sea ice, which starts in the off-shelf region, primary production is triggered by incoming solar radiation as the sun returns to the high southern latitudes. The extent of sea-ice cover in winter has a strong influence on the magnitude of primary production during the following spring/summer due to its effect on stratification and mixing (Venables et al., 2013; Schofield et al., 2017). POM is produced by phytoplankton during primary production, such that POM concentrations increase rapidly during the early part of the bloom. The production of DOC occurs at the same time, but likely at a slower net rate so that it peaks later in the growing season and continues throughout the period of increasing bacterial activity as DOC is then also being released by bacteria. As DON is produced primarily by bacterial activity, DON accumulation only starts with the development of the bacterial bloom. While there are no zooplankton biomass data available for the sampled upper ocean depths, zooplankton grazing on POM potentially contributes further to DOM production via sloppy feeding and is thus displayed

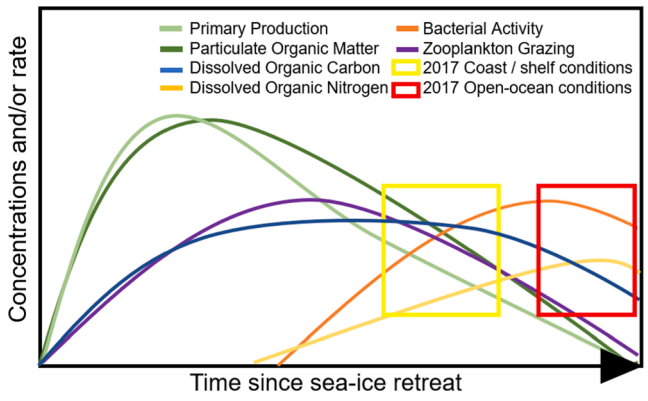

Fig. 9. Conceptual model of the progression of DOM concentrations in WAP waters in relation to a phytoplankton bloom and subsequent breakdown of organic matter by bacteria and zooplankton. The data show differences in DOC and DON concentrations due to the varying stage of the phytoplankton bloom observed at the off-shelf stations compared to the shelf and coastal stations.

in the conceptual model.

Research cruise sampling only provides a snapshot in time and thus only captures one stage of the seasonal cycle depicted by the conceptual model at each station. In 2017, in the off-shelf region, the peak of the first phytoplankton bloom likely occurred several weeks before sampling, considering the earlier retreat of sea ice in those regions, so that POM was being decomposed intensely at the time of sampling. Bacterial activity was increasing such that bacteria (as well as potentially zooplankton) were in the process of remineralising POM in the surface waters which led to increased production of bacterial DOM. Meanwhile along the coast, sampling occurred when primary production was just past its seasonal peak (Fig. 9).

This is supported by the POM and nutrient concentrations in combination with the relationships of these parameters with DOC and DON, phytoplankton and bacterial parameters, and the N isotopic compositions of PN and nitrate (see section 4.5). The phytoplankton blooms in the coastal and shelf waters occurred more recently such that both bacteria and zooplankton had had less time to react and start the decomposition process.

While this conceptual model attempts to show an overall understanding of DOM cycling in WAP shelf surface waters, the cycling of DOM, and particularly DON, is also highly sensitive to freshwater fluxes (as discussed in section 4.4) and potentially the distributions of micronutrients such as iron which play a significant role in primary production in the open Southern Ocean.

4.3. Isotopic insights into N cycling along the WAP shelf

N-isotopic signatures of nitrate ($\delta^{15}N_{NO3}$) and PN ($\delta^{15}N_{PN}$) are used here to provide additional insight into N cycle processes in the WAP shelf environment. In particular, comparison of our data with the closed system model of Rayleigh fractionation kinetics for $\delta^{15}N_{NO3}$ and the instantaneous and accumulated product equations for $\delta^{15}N_{PN}$ highlights the importance of N recycling within the context of DOM cycling described in this study (Fig. 10, see supplement I for a detailed explanation of calculations). Input parameters for the model were $[NO_3^-]_{ini}$ = 31.8 μmol L^{-1} and $\delta^{15}N_{NO3\ ini}$ = 5.5‰ taken as the mean of values measured between 75 and 125 m across the LTER grid. We use fractionation factor (ε) values of 4–6‰, consistent with ε calculated from $\delta^{15}N_{NO3}$ and $\delta^{15}N_{PN}$ (see below), as well as previous studies for the Polar Antarctic Zone and the WAP shelf region specifically (e.g. Henley et al., 2017; 2018; Difiore et al., 2010).

Good agreement between measured and modelled $\delta^{15}N_{NO3}$ is seen for the majority of samples at most stations (Fig. 10), indicating that biological uptake of the upper ocean nitrate pool by phytoplankton is the primary process influencing $\delta^{15}N_{NO3}$. Notable exceptions are observed at off-shelf stations 500.200, 400.200 and 200.200, shelf station 200.100 and coastal station 400.040, where measured values are significantly above the modelled values at intermediate depths (50–200 m). This is most likely indicating that vertical mixing is incorporating a nitrate pool that has been partially utilised into these subsurface waters (Arrigo et al., 2017; Dinniman and Klinck, 2004). Partial utilisation prior to the January cruise could have occurred in the surface ocean and/or within sea ice either *in situ* or upstream in the regional circulation; in the ACC for the off-shelf and shelf stations (Hofmann et al., 1996), or further north in the Antarctic Peninsula Coastal Current for the coastal station 400.040 (Moffat et al., 2008).

In contrast, measured values fall below the modelled relationships in surface waters at the coastal stations 600.040 and 300.040, and to a lesser degree at coastal stations 500.060 and 200.000, and shelf stations 200.100 and 200.040. Low $\delta^{15}N_{NO3}$ compared to modelled values based on nitrate uptake alone are most likely due to nitrification of low-$\delta^{15}N$ ammonium produced from the remineralisation of organic matter. This effect has been observed in numerous Southern Ocean studies and at the WAP specifically (e.g. Henley et al., 2017; 2018; Tolar et al., 2016).

The apparent ε of nitrate assimilation calculated from the slope of the regression of $\delta^{15}N_{NO3}$ versus $\ln[NO_3^-]$ (Fig. 10) can be used further to infer the importance of nitrification in lowering $\delta^{15}N_{NO3}$ (and therefore apparent ε) and resupplying the surface nitrate pool. These derived ε

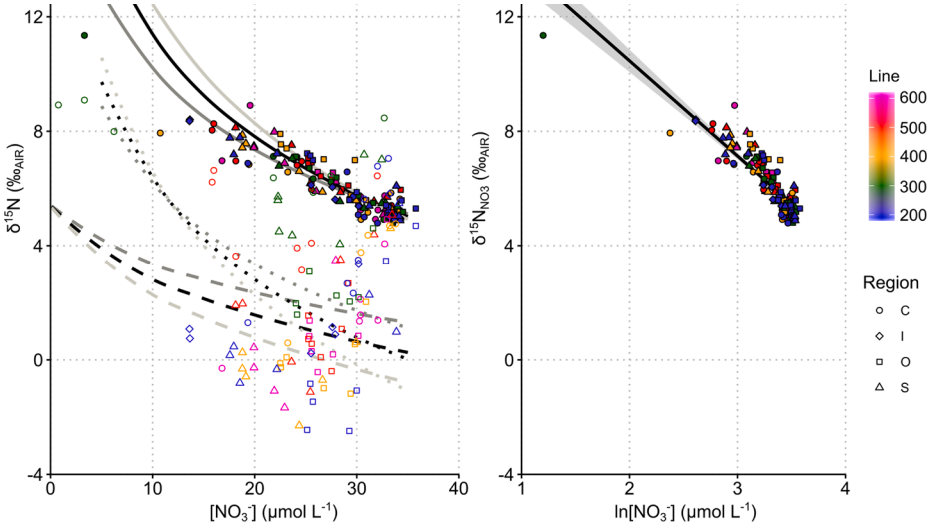

Fig. 10. Rayleigh fractionation plots of nitrate concentration vs. $\delta^{15}N$ for stations across the Palmer LTER grid in January 2017. Left hand plot shows $\delta^{15}N_{NO3}$ and $\delta^{15}N_{PN}$ vs. measured nitrate concentration, with filled symbols depicting $\delta^{15}N_{NO3}$ and open symbols depicting $\delta^{15}N_{PN}$. Trend lines are modelled values for $\delta^{15}N_{NO3}$ (solid lines) and $\delta^{15}N_{PN}$ based on the instantaneous (dotted lines) and accumulated (dashed lines) product equations. These models are based on ε of 4‰ (dark grey lines), 5‰ (black lines) and 6‰ (light grey lines). Right hand plot shows $\delta^{15}N_{NO3}$ vs. the natural log of nitrate concentration, with regression line (black) and 95% confidence intervals (grey). In both plots, symbol colour depicts sampling grid line orthogonal to the WAP coast according to the colour legend, and symbol shape denotes coastal (C), inshore (I), off-shelf (O) and shelf (S) stations according to the symbol legend.

values are between 4.2 and 6.2‰ at the majority of shelf and off-shelf stations (Table1, Supplement I), consistent with known values for nitrate assimilation by phytoplankton in the polar Southern Ocean (e.g. Difiore et al., 2010), providing further evidence for this nitrate uptake being the primary process acting on the nitrate pool. Coastal stations 500.060, 400.040, 300.040 and 200.000 and shelf stations 200.100 and 200.040 all show ε values lower than 4‰, indicating the greater importance of nitrification in inshore regions. Because nitrifiers are photo-inhibited (Hagopian and Riley, 1998), nitrification most likely takes place around the base of the euphotic layer (Fripiat, et al., 2015a; Ward, 2008) and/or in sea ice when incoming light levels are sufficiently low (Fripiat et al., 2014; 2015b). Wintertime nitrification can also modify the isotopic signature of the upper ocean nitrate pool (Smart et al., 2015), but we do not see evidence of a lowering of $\delta^{15}N_{NO3}$ in the Winter Water, suggesting that winter processes are not responsible for the upper ocean signatures shown here. It is also noteworthy that all stations over the shelf along the 200 grid line show ε values lower than 4‰, indicative of nitrification, and are situated along Marguerite Trough, a key conduit for the transport of warm nutrient-rich CDW to inshore regions. This is consistent with Henley et al. (2018) who showed the importance of nitrification in enriching this nutrient source along its flow-path through Marguerite Trough into northern Marguerite Bay, supporting the robustness of this effect over multiple years.

$\delta^{15}N_{PN}$ values also show regional patterns in N recycling, with coastal $\delta^{15}N_{PN}$ showing highest variability in accordance with both primary and bacterial production (Fig. 5). For the majority of stations, regenerated production via the utilisation of nitrified nitrate and/or low-$\delta^{15}N$ ammonium is reflected in $\delta^{15}N_{PN}$ values falling substantially below the modelled relationship for the accumulated product in the mixed layer (Fig. 10). This strongly suggests that a substantial fraction of organic matter is being recycled in the upper ocean, rather than being exported to depth, in agreement with the findings above (Section 4.3).

Below the mixed layer, most $\delta^{15}N_{PN}$ data exceed the modelled values at a number of stations, mostly at the southern stations along grid lines 200 and 300. This further supports the argument that organic matter undergoes intense decomposition over the upper ~ 100 m, which favours the lighter isotope and hence leads to increasing $\delta^{15}N_{PN}$ values below the mixed layer. These findings support those of Weston et al. (2013), who found upper-ocean recycling of particulate organic matter to be greater in Marguerite Bay in the southern part of the WAP than at Palmer Station in the northern part. The N-isotopic signatures of both nitrate and PN show more intense recycling of organic matter in the southern WAP shelf compared to the northern WAP shelf and in the coastal regions compared to shelf and off-shelf regions over the entire grid. This strongly suggests that nitrification makes a more important contribution to the surface nitrate pool in the coastal regions than further across the shelf and beyond, and more in the south than in the north of the WAP, indicating more intense biological nitrogen cycling in the upper ocean closer to the coast and further south where primary and bacterial production rates were also higher.

We have shown that a significant portion of DOC is a direct product of primary production, like POC, and therefore it is likely to undergo similarly intense recycling in the upper ocean of the WAP, as well as being generated by the subsequent decomposition of POC. DON is produced mostly by bacterial production, providing an additional recycling pathway by which organic nitrogen is remineralised to ammonium and nitrate. DON recycling is greatest in the upper ocean and in the southern part of the WAP, particularly at stations 200.000 and 400.040, where surface-water bacterial production rates are highest and DON concentrations are high at the surface and decrease rapidly with depth.

Overall, our study suggests that the production and recycling of DOC and DON in the upper ocean play a critical role in nutrient biogeochemical cycling along the WAP shelf, with DON providing an important regeneration pathway from organic matter to inorganic nutrients. Our findings support previous studies (Stukel et al., 2015; Stukel and Ducklow, 2017; Ducklow et al., 2018) that describe the WAP shelf as a high-productivity low-export environment, with organic matter remineralisation and nitrification being most intense along the coast and further south. Bacteria are shown to be the major consumers and converters of organic matter which is reflected in the relationships of bacterial abundance and activity with DON concentrations described above (Section 4.2; Fig. 8).

4.4. The influence of glacial meltwater on DOM cycling along the WAP shelf

In this study, regions subjected to strongest glacial influence (station 200.000 and 400.040 and to some extent 600.040), as shown by $\delta^{18}O_{H2O}$, also show the highest DON concentrations. The increased DON concentrations could originate directly from the glacial meltwater, or from increased bacterial activity due to the early onset of primary production and high concentrations of organic matter available for decomposition in these highly stratified waters. The latter suggestion is consistent with the exceptionally high leucine incorporation rates measured at these stations in 2017 (100–400 pmol Leu hr^{-1} L^{-1}), which were among the highest recorded during this study.

High DON concentrations could also derive from phytoplankton of a different species composition than those at the stations of lesser glacial influence, or which could be in a state of osmotic stress due to the potentially rapid decrease in salinity, triggering DON release (Hernando et al., 2015; Rijstenbil et al., 1989). At station 200.000, high DON and high bacterial activity are likely caused by a combination of recent sea-ice retreat and concurrent release of sea-ice derived organic and inorganic nutrients, sea-ice algae and bacteria, as well as the meteoric water influence (Fripiat et al., 2014). Station 400.040 also shows high concentrations of DON and bacterial activity; however, sea-ice retreat was not as recent. Here, high DON concentrations could result from high glacial influx increasing stratification and introducing nutrients as well as potentially different phytoplankton species (Annett et al., 2015; Eveleth et al., 2017) leading to relatively high primary production leading to high bacterial activity. While the rate of leucine incorporation is similar at both 200.000 and 400.040, bacterial abundance is twice as high at 200.000. This further supports the argument for a more recent addition of bacteria and DOM from both sea ice and glaciers at station 200.000.

The most prominent biological difference between the two stations is a clear difference in the bacterial community structure with 200.000 showing a ratio of HNA to LNA cells of 14.6 while at 400.040 the HNA: LNA ratio is 6.6. Even though there is much debate about what qualitative information can be drawn from HNA and LNA analyses (Gasol et al., 1999; Gomes et al., 2015; Sherr et al., 2006; Vila-Costa et al., 2012; Zubkov et al., 2001), it is clear that there is a difference which might indicate a shift in the taxonomy or physiology of the bacterial clades present (Luria et al., 2017). Bowman et al. (2017) suggested that higher HNA may represent the differences in community physiology of bacterial clades that would cycle DOM differently with varying demands for DOC and DON compounds. Compared to the other coastal stations, both 200.000 and 400.040 showed elevated HNA values and might thus express a different physiological preference for specific DOM compounds. Among all sampled stations, only station 300.040 shows a similarly high HNA:LNA ratio of 10.7 along with high glacial meltwater influx. This leads to the suggestion that the bacterial community structure is influenced by glacial meltwater input, and this is likely to have cascading effects on DOM dynamics.

DOC concentrations are also elevated at both stations 200.000 and 400.040 but not as substantially as DON concentrations. At both stations, DON and DOC concentrations decrease close to background levels within the top 50 m suggesting that the enhanced DOM is (semi)labile and is cycled rapidly by bacteria in the upper ocean, as has been discussed above.

The increased concentrations of DON in locations of high meltwater influence reveal a potential sensitivity to ongoing and future climatic

change: the majority of Antarctic Peninsula glaciers have retreated in recent decades and retreat rates are increasing, injecting increasing amounts of glacial meltwater into the ocean (Cook et al., 2005, 2015; Meredith and King, 2005), and this process is projected to continue into the future (Raphael et al., 2016). Our findings strongly suggest that these changes will lead to increased DOM concentrations in the surface waters, but a commensurate increase in bacterial rates is likely to maintain efficient cycling of DOM in the upper ocean and thus no or little export of DOM to depth. With efficient cycling of organic matter in the upper ocean and no or little export, the function of this region as a carbon sink could be affected negatively. Along with these potential changes in DOM dynamics, primary and bacterial production are highly likely to be affected by changes in glacial meltwater input, especially along the coast, with further effects on DOM production and cycling in the surface waters.

5. Conclusion

In this study, we show that DOM dynamics at the west Antarctic Peninsula are driven by a multitude of factors, with primary and bacterial production having the most direct effect on production and consumption of DOC and DON. We suggest that most DOC is produced and released directly by primary producers, as well as being produced by bacterial processing of POC, while DON is primarily a product of bacterial activity. Both dissolved organic carbon and nitrogen are cycled efficiently in the upper ocean with no or little export to greater depths. Our findings differ from previous studies that suggest that DOM is only produced by bacteria after the phytoplankton bloom, but we do show intense recycling of organic matter, especially in the coastal southern part of the WAP. Further, the $\delta^{15}N$ composition of NO_3^- and PN shows evidence for nitrification in the southern and coastal regions and to a lesser extent towards the northern and off-shelf region, also implying intense recycling of organic matter in the upper ocean with little export. In regions of high glacial meltwater influence, increased DON concentrations were found, indicating a sensitivity of DOM dynamics to variations in climate. Increasing warming and continuing melting of Antarctic glaciers could lead to an increase in DOM production, triggering a simultaneous increase in upper-ocean organic matter cycling through bacteria and hence a decrease in organic-matter export, which could negatively affect the Southern Ocean's function as a carbon sink.

Declaration of Competing Interest

The authors declare that they have no known competing financial interests or personal relationships that could have appeared to influence the work reported in this paper.

Acknowledgement

RD was funded by the UK Natural Environment Research Council (NERC) through a PhD studentship of the E3 Doctoral Training Partnership (DTP) at the University of Edinburgh. The research program was supported by a UK NERC Independent Research Fellowship awarded to SFH (NE/K010034/1). Primary production and chlorophyll data were obtained by O. Schofield, Rutgers University. Sea ice data were furnished by S. Stammerjohn, Univ Colorado-Boulder. Parts of this research were supported by NSF OPP-1440435 (Palmer LTER). Ducklow's contribution was sponsored in part by a gift from the VetlesonFoundation.

Data availability

All data are freely available from Palmer LTER (https://pal.lternet.edu/).

References

Annett, A.L., Skiba, M., Henley, S.F., Venables, H.J., Meredith, M.P., Statham, P.J., Ganeshram, R.S., 2015. Comparative Roles of Upwelling and Glacial Iron Sources in Ryder Bay, Coastal Western Antarctic Peninsula. Mar. Chem. 176, 21–33. https://doi.org/10.1016/j.marchem.2015.06.017.

Arrigo, K.R., Robinson, D.H., Worthen, D.L., Dunbar, R.B., DiTullio, G.R., VanWoert, M., Lizotte, M.P., 1999. Phytoplankton Community Structure and the Drawdown of Nutrients and CO2 in the Southern Ocean. Science 283 (5400), 365–367.

Arrigo, K.R., van Dijken, G.L., Alderkamp, A.-C., Erickson, Z.K., Lewis, K.M., Lowry, K.E., Joy-Warren, H.L., Middag, R., Nash-Arrigo, J.E., Selz, V., van de Poll, W., 2017. Early Spring Phytoplankton Dynamics in the Western Antarctic Peninsula. J. Geophys. Res. Oceans 122 (12), 9350–9369. https://doi.org/10.1002/2017JC013281.

Billen, Gilles, Becquevort, Sylvie, 1991. Phytoplankton Bacteria Relationship in the Antarctic Marine Ecosystem. Polar Res. 10 (1), 245–254. https://doi.org/10.1111/j.1751-8369.1991.tb00650.x.

Bowie, A.R., Maldonado, M.T., Frew, R.D., Croot, P.L., Achterberg, E.P., Mantoura, R.F.C., Worsfold, P.J., Law, C.S., Boyd, P.W., 2001. The Fate of Added Iron during a Mesoscale Fertilisation Experiment in the Southern Ocean. Deep-Sea Res. Part II: Topical Stud. Oceanography 48 (11–12), 2703–2743. https://doi.org/10.1016/S0967-0645(01)00015-7.

Bowman, J.S., Amaral-Zettler, L.A., Rich, J.J., Luria, C.M., Ducklow, H.W., 2017. Bacterial Community Segmentation Facilitates the Prediction of Ecosystem Function along the Coast of the Western Antarctic Peninsula. The ISME J. 11 (6), 1460–1471. https://doi.org/10.1038/ismej.2016.204.

Boyd, P.W., Ellwood, M.J., 2010. The Biogeochemical Cycle of Iron in the Ocean. Nat. Geosci. 3 (10), 675–682. https://doi.org/10.1038/ngeo964.

Boyd, P.W., Jickells, T., Law, C.S., Blain, S., Boyle, E.A., Buesseler, K.O., Coale, K.H., Cullen, J.J., de Baar, H.J.W., Follows, M., Harvey, M., Lancelot, C., Levasseur, M., Owens, N.P.J., Pollard, R., Rivkin, R.B., Sarmiento, J., Schoemann, V., Smetacek, V., Takeda, S., Tsuda, A., Turner, S., Watson, A.J., 2007. REVIEW Mesoscale Iron Enrichment Experiments 1993–2005: Synthesis and Future Directions. Science 315 (5812), 612–617.

Brown, M.S., Bowman, J.S., Lin, Y., Feehan, C.J., Moreno, C.M., Cassar, N., Marchetti, A., Schofield, O.M., 2021. Low Diversity of a Key Phytoplankton Group along the West Antarctic Peninsula. Limnol. Oceanogr. 66 (6), 2470–2480.

Carlson, C.A., Ducklow, H.W., Hansell, D.A., Smith, W.O., 1998. Organic Carbon Partitioning during Spring Phytoplankton Blooms in the Ross Sea Polynya and the Sargasso Sea. Limnol. Oceanogr. 43 (3), 375–386. https://doi.org/10.4319/lo.1998.43.3.0375.

Carlson, Craig A., Hansell, Dennis A., 2015. Chapter 3: DOM Sources, Sinks, Reactivity, and Budgets. Biogeochemistry of Marine Dissolved Organic Matter. Doi: 10.1016/B978-0-12-405940-5.00003-0.

Carlson, C.A., Hansell, D.A., Peltzer, E.T., Smith, W.O., 2000. Stocks and Dynamics of Dissolved and Particulate Organic Matter in the Southern Ross Sea, Antarctica. Deep-Sea Res. Part Ii-Topical Stud. Oceanography 47 (15-16), 3201–3225. https://doi.org/10.1016/S0967-0645(00)00065-5.

Caron, D.A., Goldman, J.C., Andersen, O.K., Dennett, M.R., 1985. 'Nutrient Cycling in a Microflagellate Food Chain: II. Mar. Ecol. Prog. Ser. 24, 243–254. https://doi.org/10.3354/meps024243.

Carter, Lionel, McCave, I.N., Williams, Michael J.M., 2008. 'Chapter 4 Circulation and Water Masses of the Southern Ocean: A Review'. Dev. Earth Environ. Sci. 8 (08): 85–114. Doi: 10.1016/S1571-9197(08)00004-9.

Casciotti, K.L., Sigman, D.M., Hastings, M.G., Bohlke, J.K., Hilkert, A., 2002. Measurement of the Oxygen Isotopic Composition of Nitrate Seawater and Freshwater Using the Dentirifier Method. Anal. Chem. 74 (19), 4905–4912.

Clarke, A., Meredith, M.P., Wallace, M.I., Brandon, M.A., Thomas, D.N., 2008. Seasonal and Interannual Variability in Temperature, Chlorophyll and Macronutrients in Northern Marguerite Bay, Antarctica. Deep-Sea Res. Part II: Topical Stud. Oceanography 55 (18–19), 1988–2006. https://doi.org/10.1016/j.dsr2.2008.04.035.

Coale, K.H., Johnson, K.S., Chavez, F.P., Buesseler, K.O., Barber, R.T., Brzezinski, M.A., Cochlan, W.P., Millero, F.J., Falkowski, P.G., Bauer, J.E., Wanninkhof, R.H., Kudela, R.M., Altabet, M.A., Hales, B.E., Takahashi, T., Landry, M.R., Bidigare, R.R., Wang, X., Chase, Z., Strutton, P.G., Friederich, G.E., Gorbunov, M.Y., Lance, V.P., Hilting, A.K., Hiscock, M.R., Demarest, M., Hiscock, W.T., Sullivan, K.F., Tanner, S.J., Gordon, R.M., Hunter, C.N., Elrod, V.A., Fitzwater, S.E., Jones, J.L., Tozzi, S., Koblizek, M., Roberts, A.E., Herndon, J., Brewster, J., Ladizinsky, N., Smith, G., Cooper, D., Timothy, D., Brown, S.L., Selph, K.E., Sheridan, C.C., Twining, B.S., Johnson, Z.I., 2004. Southern Ocean Iron Enrichment Experiment: Carbon Cycling in High- and Low-Si Waters. Science 304 (5669), 408–414.

Difiore, P.J., Sigman, D.M., Karsh, K.L., Trull, T.W., Dunbar, R.B., Robinson, R.S., 2010. Poleward Decrease in the Isotope Effect of Nitrate Assimilation across the Southern Ocean. Geophys. Res. Lett. 37 (17), 1–5. https://doi.org/10.1029/2010GL044090.

Dinniman, M.S., Klinck, J.M., 2004. A Model Study of Circulation and Cross-Shelf Exchange on the West Antarctic Peninsula Continental Shelf. Deep-Sea Res. Part II: Topical Stud. Oceanography 51 (17–19), 2003–2022. https://doi.org/10.1016/j.dsr2.2004.07.030.

Dittrich, R., 2020. The Cycling of Dissolved and Particulate Organic Matter in the Ocean West of the Antarctic Peninsula. School of GeoSciences, University of Edinburgh, Edinburgh.

Ducklow, H.W., Baker, K., Martinson, D.G., Quetin, L.B., Ross, R.M., Smith, R.C., Stammerjohn, S.E., Vernet, M., Fraser, W.R., 2007. Marine Pelagic Ecosystems: The West Antarctic Peninsula. Philos. Trans. Royal Soc. B: Biol. Sci. 362 (1477), 67–94. https://doi.org/10.1098/rstb.2006.1955.

Ducklow, Hugh W., Clarke, Andrew, Dickhut, Rebecca, Doney, Scott C., Geisz, Heidi, Huang, Kuan, Martinson, Douglas G., et al., 2012. The Marine System of the Western Antarctic Peninsula. Antarctic Ecosystems: An Extreme Environment in a Changing World, 121–59.

Ducklow, H.W., Erickson, M., Kelly, J., Montes-Hugo, M., Ribic, C.A., Smith, R.C., Stammerjohn, S.E., Karl, D.M., 2008. Particle Export from the Upper Ocean over the Continental Shelf of the West Antarctic Peninsula: A Long-Term Record, 1992–2007. Deep-Sea Res. Part II: Topical Stud. Oceanography 55 (18–19), 2118–2131. https://doi.org/10.1016/j.dsr2.2008.04.028.

Ducklow, H., Fraser, W., Meredith, M., Stammerjohn, S., Doney, S., Martinson, D., Sailley, S., Schofield, O., Steinberg, D., Venables, H., Amsler, C., 2013. West Antarctic Peninsula: An Ice-Dependent Coastal Marine Ecosystem in Transition. Oceanography 26 (3), 190–203. https://doi.org/10.5670/oceanog.2013.62.

Ducklow, H.W., Schofield, O.M.E., Vernet, M., Stammerjohn, S.E., Erickson, M., 2012b. Multiscale Control of Bacterial Production by Phytoplankton Dynamics and Sea Ice along the Western Antarctic Peninsula: A Regional and Decadal Investigation. J. Mar. Syst. 98–99, 26–39. https://doi.org/10.1016/j.jmarsys.2012.03.003.

Ducklow, H.W., Stukel, M.R., Eveleth, R., Doney, S.C., Jickells, T., Schofield, O., Baker, A.R., Brindle, J., Chance, R., Cassar, N., 2018. Spring – Summer Net Community Production, New Production, Particle Export and Related Water Column Biogeochemical Processes in the Marginal Sea Ice Zone of the Western Antarctic Peninsula 2012–2014. Phil. Trans. R. Soc. A. 376 (2122), 20170177. https://doi.org/10.1098/rsta.2017.0177.

Emery, W.J., Meincke, J., 1986. Global Water Masses: Summary and Review. Oceanol. Acta 9 (4), 383–391.

Epstein, S., Mayeda, T., 1953. Variation of O-18 Content of Waters from Natural Sources. Geochim. Cosmochim. Acta 4 (5), 213–224.

Eveleth, R., Cassar, N., Sherrell, R.M., Ducklow, H.W., Meredith, M.P., Venables, H.J., Lin, Y., Li, Z., 2017. Ice Melt Influence on Summertime Net Community Production along the Western Antarctic Peninsula. Deep-Sea Res. Part II: Topical Stud. Oceanography 139, 89–102. https://doi.org/10.1016/j.dsr2.2016.07.016.

Ferreira, Afonso, Costa, Raul R., Dotto, Tiago S., Kerr, Rodrigo, Tavano, Virginia M., Brito, Ana C., Brotas, Vanda, Secci, Eduardo R., Mendes, Carlos R.B., 2020. 'Changes in Phytoplankton Communities Along the Northern Antarctic Peninsula: Causes, Impacts and Research Priorities'. Front. Mar. Sci. 7.

Fripiat, F., Elskens, M., Trull, T.W., Blain, S., Cavagna, A.-J., Fernandez, C., Fonseca-Batista, D., Planchon, F., Raimbault, P., Roukaerts, A., Dehairs, F., 2015a. Significant Mixed Layer Nitrification in a Natural Iron-Fertilized Bloom of the Southern Ocean: NITRIFICATION IN AN IRON-FERTILIZED AREA. Global Biogeochem. Cycles 29 (11), 1929–1943. https://doi.org/10.1002/2014GB005051.

Fripiat, F., Sigman, D.M., Fawcett, S.E., Rafter, P.A., Weigand, M.A., Tison, J.-L., 2014. New Insights into Sea Ice Nitrogen Biogeochemical Dynamics from the Nitrogen Isotopes. Am. Geophys. Union. Global. Biogeochem. Cycles 28 (2), 115–130. https://doi.org/10.1002/2013GB004729.

Fripiat, F., Sigman, D.M., Masse, G., Tison, J.-L., 2015b. High Turnover Rates Indicated by Changes in the Fixed N Forms and Their Stable Isotopes in Antarctic Landfast Sea Ice. J. Geophys. Res. Oceans 120, 3079–3097. https://doi.org/10.1002/2014JC010299.Received.

Gasol, J.M., Del Giorgio, P.A., 2000. Using Flow Cytometry for Counting Natural Planktonic Bacteria and Understanding the Structure of Planktonic Bacterial Communities. Scientia Marina 64 (2), 197–224. https://doi.org/10.3989/scimar.2000.64n2197.

Gasol, J.M., Zweifel, U.L., Peters, F., Fuhrman, J.A., Hagström, Å., 1999. Significance of Size and Nucleic Acid Content Heterogeneity as Measured by Flow Cytometry in Natural Planktonic Bacteria. Appl. Environ. Microbiol. 65 (10), 4475–4483.

Ghiglione, J.F., Murray, A.E., 2012. Pronounced Summer to Winter Differences and Higher Wintertime Richness in Coastal Antarctic Marine Bacterioplankton. Environ. Microbiol. 14 (3), 617–629. https://doi.org/10.1111/j.1462-2920.2011.02601.x.

Goldman, J.C., Dennett, M.R., 2000. Growth of Marine Bacteria in Batch and Continuous Culture under Carbon and Nitrogen Limitation. Limnol. Oceanogr. 45 (4), 789–800.

Gomes, Ana, Gasol, Josep M., Estrada, Marta, Franco-Vidal, Leticia, Díaz-Pérez, Laura, Ferrera, Isabel, Morán, Xosé Anxelu G., 2015. 'Heterotrophic Bacterial Responses to the Winter-Spring Phytoplankton Bloom in Open Waters of the NW Mediterranean'. Deep-Sea Res. Part I: Oceanographic Res. Papers 96: 59–68. Doi: 10.1016/j.dsr.2014.11.007.

Gruber, N., Gloor, M., Mikaloff Fletcher, S.E., Doney, S.C., Dutkiewicz, S., Follows, M.J., Gerber, M., Jacobson, A.R., Joos, F., Lindsay, K., Menemenlis, D., Mouchet, A., Müller, S.A., Sarmiento, J.L., Takahashi, T., 2009. Oceanic Sources, Sinks, and Transport of Atmospheric CO2. Global Biogeochem. Cycles 23 (1), n/a–n/a. https://doi.org/10.1029/2008GB003349.

Hagopian, D.S., Riley, J.G., 1998. A Closer Look at the Bacteriology of Nitrification. Aquacult. Eng. 18 (4), 223–244. https://doi.org/10.1016/S0144-8609(98)00032-6.

Hansell, D.A., 2002. DOC in the Global Ocean Carbon Cycle. In: Biogeochemistry of Marine Dissolved Organic Matter. Elsevier, pp. 685–715. https://doi.org/10.1016/B978-012323841-2/50017-8.

Henley, S.F., Tuerena, R.E., Annett, A.L., Fallick, A.E., Meredith, M.P., Venables, H.J., Clarke, A., Ganeshram, R.S., 2017. Macronutrient supply, uptake and recycling in the coastal ocean of the west Antarctic Peninsula. Deep Sea Res. Part II 139, 58–76.

Henley, S.F., Jones, E.M., Venables, H.J., Meredith, M.P., Firing, Y.L., Dittrich, R., Heiser, S., Stefels, J., Dougans, J., 2018. Macronutrient and Carbon Supply, Uptake and Cycling across the Antarctic Peninsula Shelf during Summer. Philos. Trans. Royal Soc. A: Math., Phys. Eng. Sci. 376 (2122), 20170168. https://doi.org/10.1098/rsta.2017.0168.

Henley, S.F., Schofield, O.M., Hendry, K.R., Schloss, I.R., Steinberg, D.K., Moffat, C., Peck, L.S., Costa, D.P., Bakker, D.C.E., Hughes, C., Rozema, P.D., Ducklow, H.W., Abele, D., Stefels, J., Van Leeuwe, M.A., Brussaard, C.P.D., Buma, A.G.J., Kohut, J., Sahade, R., Friedlaender, A.S., Stammerjohn, S.E., Venables, H.J., Meredith, M.P., 2019. Variability and Change in the West Antarctic Peninsula Marine System: Research Priorities and Opportunities. Prog. Oceanogr. 173, 208–237. https://doi.org/10.1016/j.pocean.2019.03.003.

Hernando, M., Schloss, I.R., Malanga, G., Almandoz, G.O., Ferreyra, G.A., Aguiar, M.B., Puntarulo, S., 2015. Effects of Salinity Changes on Coastal Antarctic Phytoplankton Physiology and Assemblage Composition. J. Exp. Mar. Biol. Ecol. 466, 110–119. https://doi.org/10.1016/j.jembe.2015.02.012.

Hubberten, U., Laral, R.J., Kattnerl, G., 1995. Refractory Organic Compounds in Polar Waters : Relationship between Humic Substances and Amino Acids in the Arctic and Antarctic. J. Mar. Res. 53, 137–149. https://doi.org/10.1357/0022240953213322.

Jiao, N., Azam, F., Sanders, S., 2011. Microbial Carbon Pump in the Ocean. Science no. October.

Jiao, N., Herndl, G.J., Hansell, D.A., Benner, R., Kattner, G., Wilhelm, S.W., Kirchman, D. L., Weinbauer, M.G., Luo, T., Chen, F., Azam, F., 2010. Microbial Production of Recalcitrant Dissolved Organic Matter: Long-Term Carbon Storage in the Global Ocean. Nat. Rev. Microbiol. 8 (8), 593–599. https://doi.org/10.1038/nrmicro2386.

Klinck, J.M., Hofmann, E.E., Beardsley, R., Salihoglu, B., Howard, S., 2004. Water-Mass Properties and Circulation on the West Antarctic Peninsula Continental Shelf in Austral Fall and Winter 2001. Deep-Sea Res. Part II: Topical Stud. Oceanography 51 (17–19), 1925–1946. https://doi.org/10.1016/j.dsr2.2004.08.001.

Lechtenfeld, O.J., Kattner, G., Ruth Flerus, S., McCallister, L., Schmitt-Kopplin, P., Koch, B.P., 2014. Molecular Transformation and Degradation of Refractory Dissolved Organic Matter in the Atlantic and Southern Ocean. Geochim. Cosmochim. Acta 126, 321–337. https://doi.org/10.1016/j.gca.2013.11.009.

Lenton, A., Tilbrook, B., Law, R., Dorothée, C.E., Bakker, S.C., Doney, N., Gruber, M.H., et al., 2013. Sea-Air CO2 Fluxes in the Southern Ocean for the Period 1990–2009. Biogeosci. Discuss. 10 (1), 285–333. https://doi.org/10.5194/bgd-10-285-2013.

Li, Y., Harir, M., Lucio, M., Gonsior, M., Koch, B.P., Schmitt-Kopplin, P., Hertkorn, N., 2016. Comprehensive Structure-Selective Characterization of Dissolved Organic Matter by Reducing Molecular Complexity and Increasing Analytical Dimensions. Water Res. 106, 477–487. https://doi.org/10.1016/j.watres.2016.10.034.

Lima, Domenica Teixeira de, Moser, Gleyci A.O., Piedras, Fernanda Reinhardt, da Cunha, Leticia Cotrim, Tenenbaum, Denise Rivera, Tenorio, Marcio Murilo Barboza, de Campos, Marcos Vinicius Pereira Borges, Cornejo, Thais de Oliveira, Barrera-Alba, Jose Juan, 2019. 'Abiotic Changes Driving Microphytoplankton Functional Diversity in Admiralty Bay, King George Island (Antarctica)'. Front. Mar. Sci. 6 (638).

Lourey, M.J., Trull, T.W., Tilbrook, B., 2004. Sensitivity of Δ13C of Southern Ocean Suspended and Sinking Organic Matter to Temperature, Nutrient Utilization, and Atmospheric CO2. Deep-Sea Res. Part I: Oceanographic Res. Papers 51 (2), 281–305. https://doi.org/10.1016/j.dsr.2003.10.002.

Luria, C.M., Amaral-Zettler, L.A., Ducklow, H.W., Repeta, D.J., Rhyne, A.L., Rich, J.J., 2017. Seasonal Shifts in Bacterial Community Responses to Phytoplankton-Derived Dissolved Organic Matter in the Western Antarctic Peninsula. Front. Microbiol. 8 (November), 1–13. https://doi.org/10.3389/fmicb.2017.02117.

Marshall, G.J., Orr, A., van Lipzig, N.P.M., King, J.C., 2006. The Impact of a Changing Southern Hemisphere Annular Mode on Antarctic Peninsula Summer Temperatures. J. Clim. 19 (20), 5388–5404. https://doi.org/10.1175/JCLI3844.1.

Martinson, D.G., McKee, D.C., 2012. Transport of Warm Upper Circumpolar Deep Water onto the Western Antarctic Peninsula Continental Shelf. Ocean Sci. 8 (4), 433–442. https://doi.org/10.5194/os-8-433-2012.

Meredith, M.P., King, J.C., 2005. Rapid Climate Change in the Ocean West of the Antarctic Peninsula during the Second Half of the 20th Century. Geophys. Res. Lett. 32 (19), 1–5. https://doi.org/10.1029/2005GL024042.

Meredith, Michael P., Stammerjohn, Sharon E., Venables, Hugh J., Ducklow, Hugh W., Martinson, Douglas G., Iannuzzi, Richard A., Leng, Melanie J., Wessem, Jan Melchior van, Reijmer, Carleen H., Barrand, Nicholas E., 2016. 'Changing Distributions of Sea Ice Melt and Meteoric Water West of the Antarctic Peninsula'. Deep-Sea Research Part II: Topical Stud. Oceanography 139: 1–18. Doi: 10.1016/j.dsr2.2016.04.019.

Meredith, M.P., Venables, H.J., Clarke, A., Ducklow, H.W., Erickson, M., Leng, M.J., Lenaerts, J.T.M., Van Den Broeke, M.R., 2013. The Freshwater System West of the Antarctic Peninsula: Spatial and Temporal Changes. J. Clim. 26 (5), 1669–1684. https://doi.org/10.1175/JCLI-D-12-00246.1.

Moffat, C., Beardsley, R.C., Owens, B., van Lipzig, N., 2008. 'A first Description of the Antarctic Peninsula Coastal Current. Deep-Sea Res. Part II: Topical Stud. Oceanography 55 (3-4), 277–293.

Moline, M.A., Claustre, H., Frazer, T.K., Schofield, O.M.E., Vernet, M., 2004. Alteration of the Food Web along the Antarctic Peninsula in Response to a Regional Warming Trend. Glob. Change Biol. 10 (12), 1973–1980. https://doi.org/10.1111/j.1365-2486.2004.00825.x.

Moline, Mark a, and B B Prezelin, 1996. 'Long-Term Monitoring and Analyses of Physical Factors Regulating Variability in Coastal Antarctic Phytoplankton Composition over Seasonal and Interannual Timescales'. Mar. Ecol. Prog. Series 145: 143–60. Doi: Doi 10.3354/Meps145143.

Montes-Hugo, M., Doney, S.C., Ducklow, H.W., Fraser, W., Martinson, D., Stammerjohn, S.E., Schofield, O., 2009. Recent Changes in Phytoplankton Communities Associated with Rapid Regional Climate Change Along the Western Antarctic Peninsula. Science 323 (5920), 1470–1473.

Nikrad, M.P., Cottrell, M.T., Kirchman, D.L., Kostka, J.E., 2014. Uptake of Dissolved Organic Carbon by Gammaproteobacterial Subgroups in Coastal Waters of the West Antarctic Peninsula. Appl. Environ. Microbiol. 80 (11), 3362–3368. https://doi.org/10.1128/AEM.00121-14.

Ogawa, H., Fukuda, R., Koike, I., 1999. Vertical Distributions of Dissolved Organic Carbon and Nitrogen in the Southern Ocean. Deep-Sea Res. I 46 (10), 1809–1826. https://doi.org/10.1016/S0967-0637(99)00027-8.

Östlund, H.G., Hut, G., 1984. Arctic Ocean Water Mass Balance From Isotope Data. J. Geophys. Res. 89 (C4), 6373–6381. https://doi.org/10.1029/JC089iC04p06373.
Pereira, E.S., Garcia, C.A.E., 2018. Evaluation of satellite-derived MODIS chlorophyll algorithms in the northern Antarctic Peninsula. Deep Sea Res. Part II 149, 124–137.
Piquet, A.M.T., Bolhuis, H., Meredith, M.P., Buma, A.G.J., 2011. Shifts in Coastal Antarctic Marine Microbial Communities during and after Melt Water-Related Surface Stratification. FEMS Microbiol. Ecol. 476 (3), 413–427. https://doi.org/10.1111/j.1574-6941.2011.01062.x.
Pollard, R., Treguer, P., Read, J., 2006. Quantifying Nutrient Supply to the Southern Ocean. J. Geophys. Res. Oceans 111 (5), 1–9. https://doi.org/10.1029/2005JC003076.
Pomeroy, L., leB. Williams, P., Azam, F., Hobbie, J., 2007. The Microbial Loop. Oceanography 20 (2), 28–33. https://doi.org/10.5670/oceanog.2007.45.
Prézelin, B.B., Hofmann, E.E., Mengelt, C., Klinck, J.M., 2000. The Linkage between Upper Circumpolar Deep Water (UCDW) and Phytoplankton Assemblages on the West Antarctic Peninsula Continental Shelf. J. Mar. Res. 58 (2), 165–202. https://doi.org/10.1357/002224000321511133.
Raphael, M.N., Marshall, G.J., Turner, J., Fogt, R.L., Schneider, D., Dixon, D.A., Hosking, J.S., Jones, J.M., Hobbs, W.R., 2016. The Amundsen Sea Low: Variability, Change, and Impact on Antarctic Climate. Bull. Am. Meteorol. Soc. 97 (1), 111–121. https://doi.org/10.1175/BAMS-D-14-00018.1.
Rijstenbil, J.W., Mur, L.R., Wijnholds, J.A., Sinke, J.J., 1989. Impact of a Temporal Salinity Decrease on Growth and Nitrogene Metabolism of the Marine Diatom Skeletonema Costatum in Continuous Cultures*. Mar. Biol. 121–129.
Roobaert, A., Laruelle, G.G., Landschützer, P., Gruber, N., Chou, L., Regnier, P., 2019. The Spatiotemporal Dynamics of the Sources and Sinks of CO2 in the Global Coastal Ocean. Glob. Biogeochem. Cycles 33 (12), 1693–1714.
Rozema, P.D., Biggs, T., Sprong, P.A.A., Buma, A.G.J., Venables, H.J., Evans, C., Meredith, M.P., Bolhuis, H., 2016. Summer Microbial Community Composition Governed by Upper-Ocean Stratification and Nutrient Availability in Northern Marguerite Bay, Antarctica. Deep Sea Res. Part II no. xxxx, 1–16. https://doi.org/10.1016/j.dsr2.2016.11.016.
Russo, Arnaldo D.'Amaral Pereira Granja, Marcio Silva de Souza, Carlos Rafael Borges Mendes Mendes, Virginia Maria Tavano, Carlos Alberto Eiras Garcia, 2018. 'Spatial Variability of Photophysiology and Primary Production Rates of the Phytoplankton Communities Across the Western Antarctic Peninsula in Late Summer 2013'. *Deep Sea Research II* 149.
Saba, G.K., Fraser, W.R., Saba, V.S., Iannuzzi, R.A., Coleman, K.E., Doney, S.C., Ducklow, H.W., Martinson, D.G., Miles, T.N., Patterson-Fraser, D.L., Stammerjohn, S. E., Steinberg, D.K., Schofield, O.M., 2014. Winter and Spring Controls on the Summer Food Web of the Coastal West Antarctic Peninsula. Nat. Commun. 5 (1) https://doi.org/10.1038/ncomms5318.
Sailley, S.F., Ducklow, H.W., Moeller, H.V., 2013. Carbon Fluxes and Pelagic Ecosystem Dynamics near Two Western Antarctic Peninsula Adelie Penguin Colonies: An Inverse Model Approach. Mar. Ecol. Prog. Ser. 492, 253–272.
Sanders, R., Jickells, T., 2000. Total Organic Nutrients in Drake Passage. Deep-Sea Res. Part I: Oceanographic Res. Papers 47 (6), 997–1014. https://doi.org/10.1016/S0967-0637(99)00079-5.
Schofield, O., Saba, G., Coleman, K., Carvalho, F., Couto, N., Ducklow, H., Finkel, Z., Irwin, A., Kahl, A., Miles, T., Montes-Hugo, M., Stammerjohn, S., Waite, N., 2017. Decadal Variability in Coastal Phytoplankton Community Composition in a Changing West Antarctic Peninsula. Deep Sea Res. Part I 124, 42–54. https://doi.org/10.1016/j.dsr.2017.04.014.
Serebrennikova, Yulia M., 2005. 'Ammonium Distribution and Dynamics in Relation to Biological Production and Physical Environment in the Marguerite Bay Region of the West Antarctic Peninsula'.
Serebrennikova, Y.M., Fanning, K.A., 2004. Nutrients in the Southern Ocean GLOBEC Region: Variations, Water Circulation, and Cycling. Deep-Sea Res. Part II: Topical Stud. Oceanography 51 (17–19), 1981–2002. https://doi.org/10.1016/j.dsr2.2004.07.023.
Serebrennikova, Y.M., Fanning, K.A., Walsh, J.J., 2008. Modeling the Nitrogen and Carbon Cycling in Marguerite Bay, Antarctica: Annual Variations in Ammonium and Net Community Production. Deep-Sea Res. Part II: Topical Stud. Oceanography 55 (3–4), 393–411. https://doi.org/10.1016/j.dsr2.2007.11.009.
Sherr, E.B., Sherr, B.F., Longnecker, K., 2006. Distribution of Bacterial Abundance and Cell-Specific Nucleic Acid Content in the Northeast Pacific Ocean. Deep-Sea Res. Part I: Oceanographic Res. Papers 53 (4), 713–725. https://doi.org/10.1016/j.dsr.2006.02.001.
Sigman, D.M., Casciotti, K.L., Andreani, M., Barford, C., Galanter, M., Böhlke, J.K., 2001. A Bacterial Method for the Nitrogen Isotopic Analysis of Nitrate in Seawater and Freshwater. Anal. Chem. 73 (17), 4145–4153. https://doi.org/10.1021/ac010088e.
Sigman, D.M., Altabet M. a, D.C. McCorkle, Roger François, Fischer, G., 1999. 'The D15N of Nitrate in the Southern Ocean: Nitrate Consumption in Surface Waters'. Global Biogeochem. Cycles 13 (4): 1149–66.
Smart, S.M., Fawcett, S.E., Thomalla, S.J., Weigand, M.A., Reason, C.J.C., Sigman, D.M., 2015. Isotopic Evidence for Nitrification in the Antarctic Winter Mixed Layer. AGU Publications. Global Biogeochemical Cycles 29, 427–445. https://doi.org/10.1002/2014GB005013.Received.
Smith, D.C., Azam, F., 1992. A Simple, Economical Method for Measuring Bacterial Protein Synthesis Rates in Seawater Using Tritiated-Leucine. Mar. Microb. Food Webs 6 (2), 107–114.
Smith, R.C., Stammerjohn, S.E., Baker, K.S., 1996. Surface Air Temperature Variations in the Western Antarctic Peninsula Region. Foundations for Ecological Research West of the Antarctic Peninsula. 70, 105–121.
Soendergaard, M., Williams, P.M., Cauwet, G., Riemann, B.o., Robinson, C., Senka Terzic, E., Woodward, M.S., Worm, J., 2000. Net Accumulation and Flux of Dissolved Organic Carbon and Dissolved Organic Nitrogen in Marine Plankton Communities. Limnol. Oceanogr. 45 (5), 1097–1111. https://doi.org/10.4319/lo.2000.45.5.1097.
Stammerjohn, S.E., Martinson, D.G., Smith, R.C., Iannuzzi, R.A., 2008. Sea Ice in the Western Antarctic Peninsula Region: Spatio-Temporal Variability from Ecological and Climate Change Perspectives. Deep-Sea Res. Part II: Topical Stud. Oceanography 55 (18–19), 2041–2058. https://doi.org/10.1016/j.dsr2.2008.04.026.
Stukel, M.R., Asher, E.C., Couto, N., Oscar, M.E., Schofield, S., Strebel, P.T., Ducklow, H. W., 2015. The Imbalance of New and Export Production in the Western Antarctic Peninsula, a Potentially "Leaky" Ecosystem. Global Biogeochem. Cycles 29, 1400–1420. https://doi.org/10.1002/2015GB005211.Received.
Stukel, M.R., Ducklow, H.W., 2017. Stirring Up the Biological Pump: Vertical Mixing and Carbon Export in the Southern Ocean. Global Biogeochem. Cycles 31 (9), 1420–1434. https://doi.org/10.1002/2017GB005652.
Tagliabue, A., Sallée, J.-B., Bowie, A.R., Lévy, M., Swart, S., Boyd, P.W., 2014. Surface-Water Iron Supplies in the Southern Ocean Sustained by Deep Winter Mixing. Nat. Geosci. 7 (4), 314–320.
Takahashi, T., Sutherland, S.C., Wanninkhof, R., Sweeney, C., Feely, R.A., Chipman, D. W., Hales, B., Friederich, G., Chavez, F., Sabine, C., Watson, A., Bakker, D.C.E., Schuster, U., Metzl, N., Yoshikawa-Inoue, H., Ishii, M., Midorikawa, T., Nojiri, Y., Körtzinger, A., Steinhoff, T., Hoppema, M., Olafsson, J., Arnarson, T.S., Tilbrook, B., Johannessen, T., Olsen, A., Bellerby, R., Wong, C.S., Delille, B., Bates, N.R., de Baar, H.J.W., 2009. Climatological Mean and Decadal Change in Surface Ocean PCO2, and Net Sea-Air CO2 Flux over the Global Oceans. Deep-Sea Res. Part II: Topical Stud. Oceanography 56 (8-10), 554–577. https://doi.org/10.1016/j.dsr2.2008.12.009.
Tolar, B.B., Ross, M.J., Wallsgrove, N.J., Liu, Q., Aluwihare, L.I., Popp, B.N., Hollibaugh, J.T., 2016. Contribution of Ammonia Oxidation to Chemoautotrophy in Antarctic Coastal Waters. The ISME J. 10 (11), 2605–2619.
Tuerena, Robyn, Henley, Sian F., Dougans, Julie, Tait, Andrew, Fallick, Tony, Ganeshram, R S., 2015. 'Measuring the Stable Isotopic Composition of Nitrogen and Oxygen in Dissolved Inorganic Nitrate Using the Denitrifier Method'.
Turner, J., Hua, L.u., White, I., King, J.C., Tony Phillips, J., Hosking, S., Bracegirdle, T.J., Marshall, G.J., Mulvaney, R., Deb, P., 2016. Absence of 21st Century Warming on Antarctic Peninsula Consistent with Natural Variability. Nature 535 (7612), 1–11. https://doi.org/10.1038/nature18645.
den Meersche, V., Karel, J.J., Middelburg, K.S., Van Rijswijk, P., Boschker, H.T.S., Heip, C.H.R., 2004. Carbon-Nitrogen Coupling and Algal-Bacterial Interactions during an Experimental Bloom : Modeling a 13 C Tracer Experiment. Limnol. Oceanogr. 49 (3), 862–878.
Van Wessem, J.M., Reijmer, C.H., Berg, W.J., van den Broeke, M.R., Cook, A.J., van Ulft, L.H., van Meijgaard, E., 2015. Temperature and Wind Climate of the Antarctic Peninsula as Simulated by a High-Resolution Regional Atmospheric Climate Model. J. Clim. 28 (18), 7306–7326. https://doi.org/10.1175/JCLI-D-15-0060.1.
Vaughan, D.G., Marshall, G.J., Connolley, W.M., Parkinson, C.L., Mulvaney, R., Hodgson, D.A., King, J.C., Pudsey, C.J., Turner, J., 2003. Recent Rapid Regional Climate Warming on the Antarctic Peninsula. Clim. Change 60, 243–274. https://doi.org/10.1017/S0016756800021464.
Venables, H.J., Clarke, A., Meredith, M.P., 2013. Wintertime Controls on Summer Stratification and Productivity at the Western Antarctic Peninsula. Limnol. Oceanogr. 58 (3), 1035–1047. https://doi.org/10.4319/lo.2013.58.3.1035.
Vernet, M., Martinson, D., Iannuzzi, R., Stammerjohn, S., Kozlowski, W., Sines, K., Smith, R., Garibotti, I., 2008. Primary Production within the Sea-Ice Zone West of the Antarctic Peninsula: I - Sea Ice, Summer Mixed Layer, and Irradiance. Deep Sea Res. Part II 55 (18-19), 2068–2085.
Vila-Costa, M., Gasol, J.M., Sharma, S., Moran, M.A., 2012. Community Analysis of High- and Low-Nucleic Acid-Containing Bacteria in NW Mediterranean Coastal Waters Using 16S RDNA Pyrosequencing. Environ. Microbiol. 14 (6), 1390–1402. https://doi.org/10.1111/j.1462-2920.2012.02720.x.
Wang, X.M., Yang, G.P., Lopez, D., Ferreyra, G., Lemarchand, K., Xie, H.X., 2010. Late Autumn to Spring Changes in the Inorganic and Organic Carbon Dissolved in the Water Column at Scholaert Channel, West Antarctica. Antarct. Sci. 22 (2), 145–156. https://doi.org/10.1017/S0954102009990666.
Ward, B.B., 2008. Nitrification in Marine Systems. In: Nitrogen in the Marine Environment. Elsevier, pp. 199–261. https://doi.org/10.1016/B978-0-12-372522-6.00005-0.
Ward, B.B., Bronk, D.A., 2001. 'Net Nitrogen Uptake and DON Release in Surface Waters: Importance of Trophic Interactions Implied from Size Fractionation Experiments. Mar. Ecol. Prog. Ser. 219, 11–24.
Wessem, J.M., Van, C.H., Reijmer, W.J., De Berg, V., Van Den Broeke, M.R., Cook, A.J., Van Ulft, L.H., Van Meijgaard, E., 2015. Temperature and Wind Climate of the Antarctic Peninsula as Simulated by a High-Resolution Regional Atmospheric Climate Model. J. Clim. 28 (18), 7306–7326. https://doi.org/10.1175/JCLI-D-15-0060.1.
Weston, K., Jickells, T.D., Carson, D.S., Clarke, A., Meredith, M.P., Brandon, M.A., Wallace, M.I., Ussher, S.J., Hendry, K.R., 2013. Primary Production Export Flux in Marguerite Bay (Antarctic Peninsula): Linking Upper Water-Column Production to Sediment Trap Flux. Deep-Sea Res. Part I: Oceanographic Res. Papers 75, 52–66. https://doi.org/10.1016/j.dsr.2013.02.001.
Zubkov, M.V., Fuchs, B.M., Burkill, P.H., Amann, R., 2001. Comparison of Cellular and Biomass Specific Activities of Dominant Bacterioplankton Groups in Stratified Waters of the Celtic Sea. Appl. Environ. Microbiol. 67 (11), 5210–5218. https://doi.org/10.1128/AEM.67.11.5210.

Further reading

Ducklow, H.W., 2009. Southern Ocean: Biogeochemistry. In 41, 1–5. https://doi.org/10.1126/science.1247727.